12-1-2012

STUDY OF PARTICLE SWARM FOR OPTIMAL POWER FLOW IN IEEE BENCHMARK SYSTEMS INCLUDING WIND POWER GENERATORS

Mohamed A. Abuella
Southern Illinois University Carbondale, mohammedabuella@siu.edu

STUDY OF PARTICLE SWARM FOR OPTIMAL POWER FLOW IN IEEE BENCHMARK SYSTEMS INCLUDING WIND POWER GENERATORS

by

Mohamed A. Abuella

B.Tech., Higher Institute of Industry, Misurata, Libya 2008

A Thesis
Submitted in Partial Fulfillment of the Requirements for the
Master of Science Degree

Department of Electrical and Computer Engineering
in the Graduate School
Southern Illinois University Carbondale
December, 2012

THESIS APPROVAL

STUDY OF PARTICLE SWARM FOR OPTIMAL POWER FLOW IN IEEE BENCHMARK SYSTEMS INCLUDING WIND POWER GENERATORS

By

Mohamed A. Abuella

A Thesis Submitted in Partial

Fulfillment of the Requirements

for the Degree of

Master of Science

in the field of Electrical and Computer Engineering

Approved by:

Dr. Constantine J. Hatziadoniu, Chair

Dr. Farzad Pourboghrat

Dr. Dimitrios Kagaris

Graduate School
Southern Illinois University Carbondale
May 10, 2012

AN ABSTRACT OF THE THESIS OF

Mohamed A. Abuella, for the Master of Science degree in Electrical and Computer Engineering, presented on May 10, 2012, at Southern Illinois University Carbondale.

TITLE:STUDY OF PARTICLE SWARM FOR OPTIMAL POWER FLOW IN IEEE BENCHMARK SYSTEMS INCLUDING WIND POWER GENERATORS

MAJOR PROFESSOR: Dr. C. Hatziadoniu,

The aim of this thesis is the optimal economic dispatch of real power in systems that include wind power. The economic dispatch of wind power units is quite different of conventional thermal units. In addition, the consideration should take the intermittency nature of wind speed and operating constraints as well. Therefore, this thesis uses a model that considers the aforementioned considerations in addition to whether the utility owns wind turbines or not. The optimal power flow (OPF) is solved by using one of the modern optimization algorithms: the particle swarm optimization algorithm (PSO).

IEEE 30-bus test system has been adapted to study the implementation PSO algorithm in OPF of conventional-thermal generators. A small and simple 6-bus system has been used to study OPF of a system that includes wind-powered generators besides to thermal generators.

The analysis of investigations on power systems is presented in tabulated and illustrative methods to lead to clear conclusions.

DEDICATION

I dedicate this modest work to my family. My father, mother and siblings.

ACKNOWLEDGMENTS

I would like to thank Dr. Hatziadoniu for his invaluable assistance and insights leading to the writing of this thesis. My sincere thanks also goes to the members of Electrical and Computer Engineering for their patience and understanding during the two years of effort that went into the production of this work.

A special thanks also to my friends. Another special thanks to Libyan Higher Education Ministry for awarding me a scholarship to study abroad.

TABLE OF CONTENTS

LIST OF TABLES

LIST OF FIGURES

CHAPTER 1

INTRODUCTION

1.1 THE MOTIVATION

1.1.1 The Growing Importance of Wind Energy

With increasing fuel prices and environmental concerns, many governments have supported research on renewable energy applications under the consideration of diversifying energy sources. Among the various renewable energy sources, wind energy could be one of the most promising renewable energy sources[1].

From the birth of modern electricity-generating wind turbines in the late 1970s to now, wind energy technology has dramatically improved. Capital costs have decreased, reliability has improved, and efficiency has increased. High-quality turbine manufacturers exist around the world, and wind plants of 300 MW and larger are being integrated into the electrical grid to exacting utility specifications. These modern wind plants are now routinely produced by multinational manufacturing companies at less cost and high energy efficiency [2].

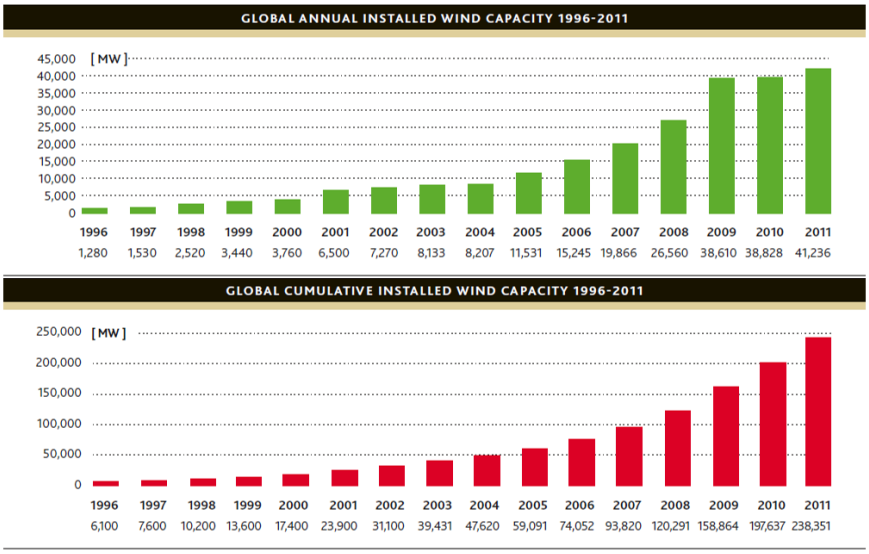

Figure 1.1: Global Installed Wind Capacity 1996-2011[3]

1.1.2 The Cost of Wind Energy

In contrast to the uncertainties surrounding supplies of conventional fuels, and volatile prices, wind energy is a massive indigenous power source which is permanently available in virtually every country in the world. Other than new gas, coal or even nuclear power plants, the price for fuel over the total lifetime of a wind turbine is well known; it is zero. For conventional generation technologies, the volatility of fuel price developments are a significant risk factor, with oil prices recently (2012) fluctuating between 50 and 150 USD in the course of just one year[4].

Wind farm owners, however, know how much the electricity they generate is going to cost. No conventional technology (except hydro) can make that claim. This is of fundamental interest not only to individual utilities and power plant operators, but also to government planners seeking to mitigate their vulnerability to macroeconomic shocks associated with the vagaries of international commodity markets.

In addition, at many sites, wind power is already competitive with new-built conventional technologies, and in some cases much cheaper. Although nothing can compete with existing, embedded conventional generation plant that has already been paid off (and was mostly constructed with significant state subsidies: governments still subsidize conventional technologies at the rate of about 250 billion USD/year), wind power is commercially attractive, especially when taking into account the price of carbon, which is a factor in a growing number of markets[4]. For more information on the cost of wind energy, see reference[5].

1.1.3 The Optimal Economic Dispatch of Wind Power

The optimal power dispatch for the system that includes wind power generators is the subject of ongoing research model nowadays. So that, this thesis considers an optimal power flow (OPF) of wind-thermal units coordination.

In general, the problem with wind power is the stochastic nature of wind speed.

Therefore the model which considers the probability of the available wind power can represent the cost of overestimating and underestimating this power at a certain period of time. In addition, there is a different penalty cost factor for wind power generators whether they are owned or not owned by the utility [6].

The particle swarm optimization (PSO) technique is one of the modern heuristic algorithms for solving the optimization problem. The endless increasing development in computers and their softwares played a key role in prosperity of this optimization technique. As a result, PSO has been used widely in many applications. So that PSO can be a good choice for solving the optimal power flow for the system of wind and thermal generators [7],[8]. Especially, for a model that has a non-linear objective function besides to integrations for the penalty costs.

1.2 STATEMENT OF THE PROBLEM

1.2.1 Problem Formulation

Optimal economic dispatch is an optimization problem to find the optimal allocation of output power among the available generators with given constraints. This optimal allocation depends on various factors, such as operating cost, system security (or risk) and CO_2 emissions, in general they are called cost factors.

The objective function of the optimization problem in the thesis is to minimize the operating cost of real power generation.

The objective function and the constraints are mostly nonlinear and many methods and algorithms have been developed on the basis of cost factors; generation source type, conventional or renewable; uncertainty treatment (i.e. deterministic or stochastic). For instance, Lagrangian relaxation, direct search method, evolution programming, particle swarm optimization, genetic algorithms, and simulated annealing are some of the solution methods for economic dispatch optimization problem [9].

The main problem of the optimal economic dispatch which includes wind power is the

unpredictability or the uncertainty of the wind power. Therefore, the stochastic nature of wind affects the economic dispatch.

1.2.2 Problem objectives

The objective of the problem is the minimization of the total cost of real power generation. The operating cost of conventional thermal generators is represented by a quadratic equation as following[10],[11]:

$$C_i = a_i p_i^2 + b_i p_i + c_i \tag{1.1}$$

Where p_i is the generation power from the $\boldsymbol{i}$th conventional generator; and a, b and c are the operating cost coefficients of the $\boldsymbol{i}$th generator.

The wind power generation cost which may be not exist if the power operator owns the wind powered-generators, but it could be considered as a payback cost or a maintenance and renewal cost[12]:

$$C_{w,i} = d_i w_i \tag{1.2}$$

Since w_i is the scheduled wind power from the $\boldsymbol{i}$th wind-powered generator; and d_i is the direct cost coefficient for the ith wind generator.

Because the wind speed has an uncertainty nature so that the generated wind power will be uncertain as well. As it is shown in figure(1.2), which shows the variation of available wind power W_{av} from the scheduled wind power w_i at certain period of time. The surplus of wind power which is more than the scheduled wind power w_i has a cost, especially when the utility doesn't have its own wind turbines. At that time the surplus of wind power which is not used should be paid to the operator that owns the wind turbines.

On the other hand, a deficit of wind power which occurs when the available wind power less than the scheduled wind power w_i. In that situation the required power will be supplied or compensated by a reserve power sources such us energy storing systems or standby generators. That means there is also a cost for the deficit of wind power.

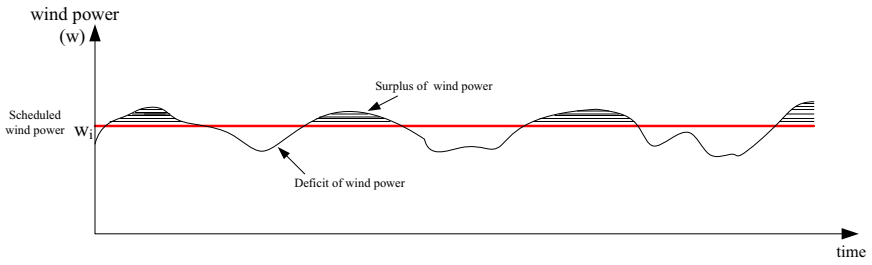

Figure 1.2: The variation of available wind power during a particular period of time

Therefore, the penalty cost for not using all available wind power at certain period of time is:

$$C_{p,i} = k_{p,i} \int_{w_i}^{w_{r,i}} (w - w_i) f_w(w) dw \tag{1.3}$$

Where f_w is the Weibull distribution function for wind speeds after it has been transformed to wind power, it will be discussed by some details in section (2.1.2); and $k_{p,i}$ is the penalty cost coefficient for the $\boldsymbol{i}$th wind generator, it appears as a result of underestimation of available wind power;

In similar fashion, the reserve cost represents the reserve power if the scheduled wind power is not sufficient in certain period of time:

$$C_{r,i} = k_{r,i} \int_{0}^{w_i} (w_i - w) f_w(w) dw \tag{1.4}$$

Since $k_{r,i}$ is the reserve cost coefficient for the $\boldsymbol{i}$th wind generator, it appears as a result of overestimation of available wind power.

1.2.3 Problem Constraints

Due to the physical or operational limits in practical systems, there is a set of constraints that should be satisfied throughout the system operations for a feasible solution [13].

- Generation capacity constraints:

For normal system operations, real power output of each generator is restricted by lower and upper limits as follows:

$$p_i^{min} \leq p_i \leq p_i^{max} \tag{1.5}$$

$$0 \leq w_i \leq w_{r,i} \tag{1.6}$$

Since $w_{r,i}$ is the rated wind power from the $\boldsymbol{i}$th wind-powered generator;

- Power balance constraint:

  The total power from conventional and wind generators must cover the total demand.

$$\sum_{i=1}^{M} p_i + \sum_{i=1}^{N} w_i = L \tag{1.7}$$

  Where M number of conventional power generators; N number of wind-powered generators; and L is the system load and losses.

- Operating constraints:

$$V_i^{min} \leq V_i \leq V_i^{max} \tag{1.8}$$

$$S_{line,i} \leq S_{line,i}^{max} \tag{1.9}$$

  V_i is the magnitude of voltage at the $\boldsymbol{i}$th bus; $S_{line,i}$ is the rating of the $\boldsymbol{i}$th transmission line.

1.2.4 Problem Statement

In summary, the objectives of optimal economical dispatch is to minimize the operating cost from the conventional and wind-powered generators includes the penalty of underestimation and overestimation of wind power, subject to the certain constraints.

The model of economic dispatch for thermal and wind-powered generators[12]:

$$\sum_{i=1}^{M} C_i(p_i) + \sum_{i=1}^{N} C_{w,i}(w_i) + \sum_{i=1}^{N} C_{p,i}(w_i) + \sum_{i=1}^{N} C_{r,i}(w_i) \tag{1.10}$$

subject to:

$$p_i^{min} \leq p_i \leq p_i^{max}$$

$$0 \leq w_i \leq w_{r,i}$$

$$\sum_{i=1}^{M} p_i + \sum_{i=1}^{N} w_i = L$$

$$V_i^{min} \leq V_i \leq V_i^{max}$$

$$S_{line,i} \leq S_{line,i}^{max}$$

Note using a classic economic dispatch approach for the model in equation (1.10), which takes the partial derivative of the objective function respect to generator outputs; it's difficult due to the integrals in the wind power cost terms as in equations (1.3) and (1.4), Therefore, Particle Swarm Optimization (PSO) algorithm has been used for solving this optimization problem [14], [15].

1.3 LITERATURE REVIEW

Optimal power flow (OPF) is regarded as the backbone tool that has been extensively researched since its first introduction. It deals with the minimum cost of power production in electrical power system analysis with certain constraints[11],[15].

In the literature, the OPF problem has been investigated from different aspects. Some researchers paid attention to seeking efficient algorithms The studies about OPF methods can be traced back to the 1960s when France scholar Carpentier and Siroux firstly discussed the OPF problem, and then H.W. Domme and W.F.Tinnety presented a simplified derivative algorithm which is the first practicable algorithm for OPF problem [16]. But in this algorithm there will appear vibration phenomenon when it is closing to the optimum.

Since then, various kinds of mathematical programming approaches, based on linear and nonlinear programming were proposed in succession, including Newton method, quadratic programming, and interior-point method [16]. All these aforementioned methods utilize first or second derivative information in essence. In this way, it is apt to fall into local optima. Furthermore, there is a difficulty of applying gradient-based optimization techniques to solve OPF including wind generators. Therefore, various non-classical

optimization methods have emerged to cope with some of the traditional optimization algorithms' shortcomings [12].

The main modern optimization techniques are genetic algorithm (GA), evolutionary programming (EP), artificial neural network (ANN), simulated annealing (SA), ant colony optimization (ACO), and particle swarm optimization (PSO). Most of these relatively new developed algorithms mimic a certain natural phenomenon in its search for an optimal solution like species evolution (GA and EP), human neural system (ANN), thermal dynamics of a metal cooling process (SA), or social behavior (ACO and PSO). They have been successfully applied to wide range of optimization problems in which global solutions are more preferred than local ones [17],[18].

Kennedy and Eberhart first introduced particle swarm optimization (PSO) in 1995 as a new heuristic method [19]. In [18] there is a comprehensive coverage of different PSO applications in solving optimization problems in the area of electric power systems up to 2006. PSO has been successfully used to solve the OPF problem, but the approach usually suffers a major difficulty in how to properly select penalty factor value for the constraints.

Abido introduced PSO to solve the OPF problem [20]. In OPF, the goal is to find the optimal settings of the control variables such that the sum of all generators' cost functions is minimized. The generator real power outputs are considered as control variables in addition to the other control variables.

One purpose of this thesis is to use the PSO algorithm to solve OPF problem.

The helpful references [21], [22] have explanations about the mechanism of applying PSO for solving optimal power flow problem.

The review in [23] is about the historical research production of the economic dispatch considering the wind power, besides that it also presents some models and different optimization algorithms as well.

In 2008 one of the pioneer studies [12] about economic dispatch including the wind power was reported. It also includes the definitions about the wind power cost and its

factors in wind energy conversion systems (WECS) combining both cases, the operator owns WECS or not. In addition to the direct cost of wind power, cost factors of the overestimation and underestimation of wind power have also been proposed.

Several investigations have looked at the prediction of wind speed for use in determining the available wind power. These investigations have been based on such foundations as fuzzy logic [24], neural networks [25], and time series [26].

In [27] and [12], the model uses the probability and stochastics of wind power availability to solve optimal economic dispatch problem.

A comprehensive review for probability distributions of wind speed can be found in [28], where the authors cited more than two hundred publications and described more than ten well-known distributions. They indicated that the two-parameter Weibull distribution had become the most widely accepted model and had been included in regulatory works as well as several popular computer modeling packages [29].

A known Weibull probability distribution function (PDF) for the wind speed has been used, and then, transformed to the corresponding wind power distribution for use in the model [12]. Moreover, [12] indicates the advantages of selecting Weibull probability distribution function of wind power.

The used model in the thesis is based on the Weibull probability distribution of wind speed, and a linear transformation of wind speed probability distribution function to wind power probability distribution function.

The sensitivity analysis of OPF is used in selecting control variables that have most effect on state variables. This idea is useful in adjusting violations in operating constraints of the power system by using less number of control variables. The fundamentals of sensitivity analysis of OPF can be found in references such as [30], [31], and [32].

1.4 OUTLINE OF THE THESIS

The thesis is organized as follows:

Chapter 1 introduces the motivation, the problem statement, the literature review and the outlet of the thesis.

Chapter 2 in the beginning, it discusses the characterization of wind speed as a random variable and will introduce the Weibull probability density function. The power input-output equation of the wind energy conversion systems (WECS) and the transformation from the wind speed random variable to the wind power random variable is presented as well. The basics of optimal power flow (OPF) is also included.

Chapter 3 the particle swarm optimization (PSO) algorithm is introduced with its parameters and its mechanism is also explained.

Chapter 4 consists the study cases of test systems, 30 bus test system and 6 bus test system which contains wind generators, there is analysis of simulation results as well.

Chapter 5 sums-up conclusions and suggests a further work.

CHAPTER 2

OPTIMAL POWER FLOW INCLUDING WIND-POWERED GENERATORS

2.1 PROBABILITY ANALYSIS OF WIND POWER

Before starting the discussion of optimal power flow of systems that contain wind-powered generators, it will be a good idea to identify the wind speed characterization by probability principles and its subsequent transformation to wind power.

2.1.1 Wind Speed Characterization

The wind speeds in a particular place take a form of Weibull distribution over time [28, 33]. The probability density function (pdf) of the Wiebull distribution is given by:

$$f_V(v) = \left(\frac{k}{c}\right)\left(\frac{v}{c}\right)^{(k-1)}\ e^{-(\frac{v}{c})^k}, \qquad 0 < v < \infty \tag{2.1}$$

Where $f_V(v)$ is the pfd of wind speed; v is the wind speed; c is scale factor; k is the shape factor.

Figure (2.1) illustrates the Weibull pdf with shape factors k=2, and curves of scale factor $c = 5$, 15, and 25 are indicated.

Here some comments on figure (2.1) can be made.

The mean of the Weibull function is:

$$\mu = c\Gamma(1 + k^{-1}) \tag{2.2}$$

While the variance (standard deviation) is:

$$\sigma_v^2 = c^2\Gamma(1 + 2k^{-1}) - \mu^2 \tag{2.3}$$

Where Gamma function Γ is:

$$\Gamma(x) = \int_0^\infty y^{x-1}\ e^{-y} dy \tag{2.4}$$

When k=2 this is a special case of Weibull pdf it is called Rayleigh distribution. At which the mean and the variance are:

$$\mu = c\frac{\sqrt{\pi}}{2}, \qquad \sigma_v^2 = c^2(1 - \frac{\pi}{4}) \tag{2.5}$$

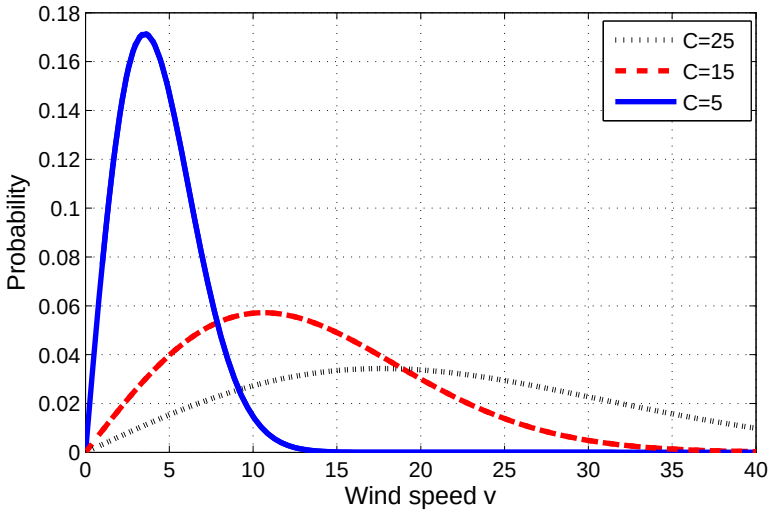

Figure 2.1: Weibull pdf of wind speed for several values of scale factor c [33]

The cumulative distribution function (cdf) of Weibulll distribution is obtained by integration of pdf:

$$F_V(v) = \int_0^v f_V(v)\, dv = 1 - e^{-(\frac{v}{c})^k} \tag{2.6}$$

$F_V(v)$ is Weibull cumulative distribution. Figure (2.2) shows Weibull pdf and cdf distribution functions of wind speed when c=5.

It is seen that, as the c factor of the Weibull function increases, the mean and standard deviation also increase in a linear relationship.

The advantages of the Weibull distribution are noted as follows [12]:

1. It is a two parameter distribution, which is more general than the single parameter Rayleigh distribution, but less complicated than the five-parameter bivariate normal distribution;

2. It has been previously shown to provide a good fit to observed wind speed data;

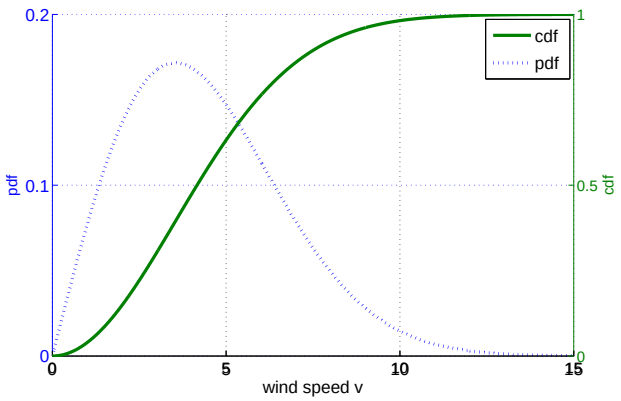

Figure 2.2: Weibull pdf and cdf of wind speed for c=5

3. If the k and c parameters are known at one height, a methodology exists to find the corresponding parameters at another height.

The characteristics of the wind depend on various factors like geography, topography, etc., and can be estimated by the observed frequency of wind speed in the target region.

2.1.2 WECS Input/Output and Probability Functions

The captured power output of the wind turbine can be written as [33],

$$P_m = C_p \frac{\rho}{2} A_R v^3 \tag{2.7}$$

Where, ρ is air density of the site, v is wind speed, A_R is sectional area of the turbine, and $C_p(\lambda, \beta)$ is power coefficient depends on the tip speed ratio λ and the pitch angle β:

$$\lambda = \frac{\omega.R}{v} \tag{2.8}$$

Where R and ω are radius and rotational speed of the wind turbine respectively.

As it is shown in figure (2.3), the wind power from probability point of view can be represented in three regions as in equation (2.9). When wind speed is $(v_i \leq v < v_r)$, the captured wind power can be represented as a linear relationship with the wind speed in wind energy conversion systems (WECS) by ignoring the minor nonlinearity. So that the

wind power curve is assumed to be linear as following [14, 12]:

$$w = \begin{cases} 0; & (v < v_i \ or \ v \geq v_o) \\ w_r \frac{(v - v_i)}{(v_r - v_i)}; & (v_i \leq v < v_r) \\ w_r; & (v_r \leq v < v_o) \end{cases} \tag{2.9}$$

Where w is the wind power; w_r is the rated power of WECS; v_i is the cut-in wind speed; v_o is the cut-out of wind speed; v_r is the rated wind speed at which the rated power w_r is captured.

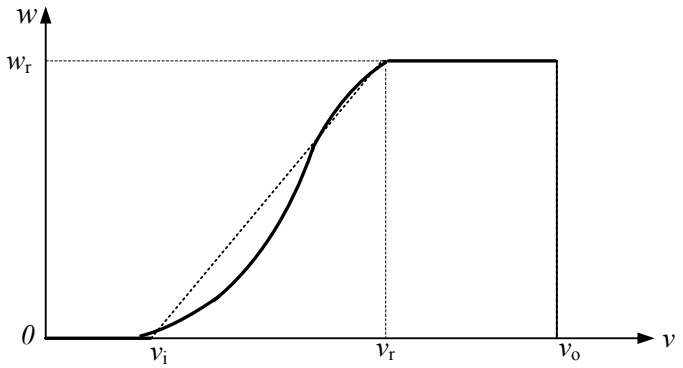

Figure 2.3: The captured wind power curve [33]

The linear transformation from wind speed to wind power in the linear region $(v_i \leq v < v_r)$ is done as following [12]:

$$\because w = T(v) = av + b$$

So now v in terms of w as follows:

$$\therefore v = T^{-1}(w) \Rightarrow v = \frac{(w - b)}{a}$$

$$f_W(w) = f_V(T^{-1}(w)) \left[\frac{dT^{-1}(w)}{dw} \right]$$

$$\therefore f_W(w) = f_V \left(\frac{w - b}{a} \right) \left| \frac{1}{a} \right| \tag{2.10}$$

where:

T is the general transformation; w wind power random variable; v wind speed random variable;

For Weibull distribution function, the transformation will lead to discrete and continuous ranges as following: For discrete portions:

$$Pr\{W = 0\} = F_V(v_i) + (1 - F_V(v_o))$$
$$Pr\{W = 0\} = 1 - e^{-(\frac{v_i}{c})^k} + e^{-(\frac{v_o}{c})^k} \tag{2.11}$$

and

$$Pr\{W = w_r\} = F_V(v_o) - F_V(v_r)$$
$$Pr\{W = w_r\} = -e^{-(\frac{v_r}{c})^k} - e^{-(\frac{v_o}{c})^k} \tag{2.12}$$

While for the continuous portion (i.e. linear portion of wind power curve):

$$\rho = \frac{w}{w_r}$$
$$l = \frac{(v_r - v_i)}{v_i}$$
$$f_W(w) = \frac{klv_i}{w_r c}\left(\frac{(1+\rho l)v_i}{c}\right)^{(k-1)} e^{-\left(\frac{(1+\rho l)v_i}{c}\right)^k} \tag{2.13}$$

Wind power output mixed (i.e. discrete and continuous portions) probability function for the Weibull pdf of wind speeds is shown in figure (2.4).

As it is shown, the discrete probabilities at $\frac{w}{w_r} = 0$ and $\frac{w}{w_r} = 1$ are illustrated by individual markers of constant values which derived from equations (2.11, 2.12), while the continuous probability function occurs when $0 < \frac{w}{w_r} < 1$ yielded from direct substitution in equation (2.13), and these continuous portions of the probability function may be associated with the corresponding discrete probability markers shown at both ends of the probability function. For figure (2.4), the shape factor k=2, and for a wind turbine with v_i =5 mi/hr, v_r= 15 mi/hr, and v_o = 45 mi/hr [12].

As the c factor in the Weibull distribution function is increased, a greater proportion of the wind speed profile will be located at higher values of wind speed (as shown in figure

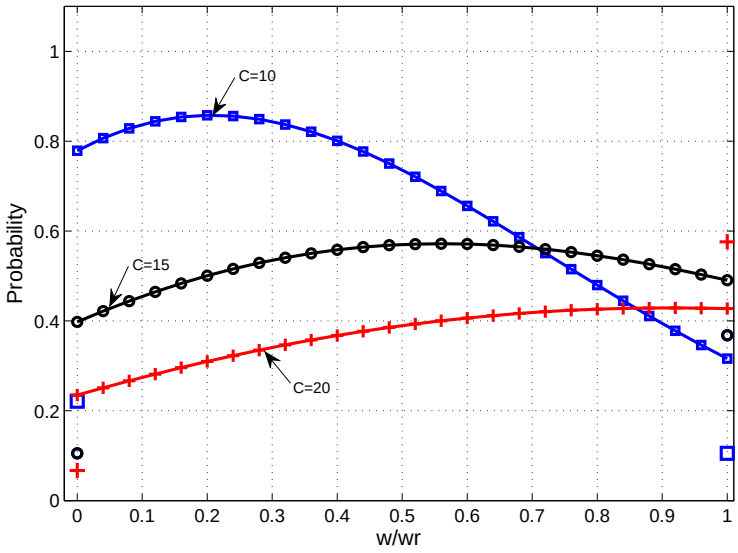

Figure 2.4: Probability vs. Wind power for C=10, 15 and 20 [12]

(2.1)). This translates to a lower discrete probability of zero power, a higher discrete probability of rated power, and less power in the continuous portion of the plot. As with any other mixed discrete and continuous probability function, the sum of the discrete probabilities at zero and rated power, plus the integral from 0 to 1 ($0 < \frac{w}{w_r} < 1$) of the continuous function will sum to 1.

2.2 OPTIMAL POWER FLOW

The optimal power flow (OPF) is a mathematical optimization problem set up to minimize an objective function subject to equality and inequality constraints.

In the past two decades, the problem of optimal power flow (OPF) has received much attention. The OPF problem solutions aims to optimize a selected objective function such as the system operating cost via adjustment of the power system control variables, while at the same time satisfying various equality and inequality constraints [20].

The equality constraints are the power flow equations, while the inequality constraints are the limits on control variables and the operating limits of power system dependent

(state) variables. The problem control variables include the generator real power, the generator bus voltages, the transformer tap settings, and the reactive power of switchable VAR sources. On the other hand, the problem dependent variables include the load bus voltages, the generator reactive powers, and the line flows. Generally, the OPF problem is a large-scale highly constrained nonlinear nonconvex optimization problem.

Mathematically, the OPF problem can be formulated as follows:

$$Min \quad J(\mathbf{x},\mathbf{u}) \tag{2.14}$$

Subject to:

$$g(\mathbf{x},\mathbf{u}) = 0 \tag{2.15}$$

$$h(\mathbf{x},\mathbf{u}) \leq 0 \tag{2.16}$$

Where J is the objective function to be minimized, it could be the cost of real power of thermal units, wind-powered units, or mix of them. g is the equality constraints represent the power flow equations. h is the inequality constraints that represent the operating limits of the system.

Where $g(\mathbf{x},\mathbf{u}) = 0$ are the balanced power flow equations as following:

$$P_i - V_i \sum_{j=1}^{n} V_j Y_{ij} \cos(\delta_i - \delta_j - \theta_{ij}) = 0 \tag{2.17}$$

$$Q_i - V_i \sum_{j=1}^{n} V_j Y_{ij} \sin(\delta_i - \delta_j - \theta_{ij}) = 0 \tag{2.18}$$

Where P_i is the specified real power at bus i, and it equals to the difference between the generation and demand load real power (P_{Gi}-P_{Di}) at bus i, and the same for Q_i; Y_{ij} is the admittance between buses i and j;V_i is the voltage magnitude of bus i; and δ_i is the phase angle of the voltage at bus i.

In equations (2.14-2.16), $\mathbf{x}$ is the vector of dependent (state) variables consisting of slack bus power P_{G1}, load bus voltages V_L, generator reactive power output Q_G, and transmission line ratings (loadings) S_{line}. Here x can be expressed as:

$$\mathbf{x}^T = [P_{G_1},\, V_{L_1}...V_{L_{NL}},\, Q_{G_1}...Q_{G_{NG}},\, S_{line_1}...S_{line_{nl}}] \tag{2.19}$$

Where NL, NG, and nl are number of load buses, number of generators, and number of transmission lines respectively.

$\mathbf{u}$ is the vector of independent (control) variables consisting of generator voltages V_G, generator real power outputsP_G except the slack bus P_{G1}, transformer tap settings T, and shunt VAR compensations Q_C.

Hence, $\mathbf{u}$ can be expressed as:

$$\mathbf{u}^T = [V_{G_1}...V_{G_{NG}},\, P_{G_2}...P_{G_{NG}},\, T_1...T_{NT},\, Q_{C_1}...Q_{C_{NC}}] \tag{2.20}$$

Where NT and NC are the number of the regulating transformers and shunt compensators respectively.

- Generating constraints:

  Generator voltages, real power outputs, and reactive power outputs are restricted by their lower and upper limits as follows:

$$V_{G_i}^{min} \leq V_{G_i} \leq V_{G_i}^{max}, \qquad i = 1, ..., NG \tag{2.21}$$

$$P_{G_i}^{min} \leq P_{G_i} \leq P_{G_i}^{max}, \qquad i = 1, ..., NG \tag{2.22}$$

$$Q_{G_i}^{min} \leq Q_{G_i} \leq Q_{G_i}^{max}, \qquad i = 1, ..., NG \tag{2.23}$$

- Transformer constraints:

  Transformer tap settings are bounded as follows:

$$T_i^{min} \leq T_i \leq T_i^{max}, \qquad i = 1, ..., NT \tag{2.24}$$

- Shunt VAR constraints:

  Shunt VAR compensations are restricted by their limits as follows:

$$Q_{C_i}^{min} \leq Q_{C_i} \leq Q_{C_i}^{max}, \qquad i = 1, ..., NC \tag{2.25}$$

- Security constraints:

  These include the constraint of voltages at load buses and the transmission line loadings as follows:

$$V_{L_i}^{min} \leq V_{L_i} \leq V_{L_i}^{max}, \qquad i = 1, ..., NL \tag{2.26}$$

$$S_{line_i} \leq S_{line_i}^{max}, \qquad i = 1, ..., nl \tag{2.27}$$

It is worth to mention that the control variables are self-constrained. The hard inequalities of P_{G_1}, V_L, Q_G, and S_{line} can be incorporated in the objective function as quadratic penalty terms (penalty functions). Therefore, the objective function in equation (2.14) can be augmented as follows:

$$J_{aug} = J + \lambda_P (P_{G_1} - P_{G_1}^{lim})^2 + \lambda_V \sum_{i=1}^{NL} (V_{L_i} - V_{L_i}^{lim})^2 + \lambda_Q \sum_{i=1}^{NG} (Q_{G_i} - Q_{G_i}^{lim})^2 + \lambda_S \sum_{i=1}^{nl} (S_{line_i} - S_{line_i}^{max})^2 \tag{2.28}$$

Where λ_P, λ_V, λ_Q, and λ_S are penalty factors and x^{lim} is the limit value of the dependent variable x given as:

$$x^{lim} = \begin{cases} x^{max}; & (x > x^{max}) \\ x^{min}; & (x < x^{min}) \end{cases} \tag{2.29}$$

CHAPTER 3

PARTICLE SWARM OPTIMIZATION

3.1 INTRODUCTION

The original PSO suggested by Kennedy and Eberhart is based on the analogy of swarm of bird and school of fish [19]. The algorithm was simplified and it was observed to be performing optimization.

It uses tools and ideas taken from computer graphics and social psychology. The rules that govern the movement of the particles in a problem's search space can also be seen as a model of human social behavior in which individuals adjust their beliefs and attitudes to conform with those of their peers [19]. The PSO optimizes a problem by iteratively trying to improve a candidate solution with regard to a given measure of quality.

3.2 STANDARD ALGORITHM

PSO, as an optimization tool, provides a swarm-based search procedure in which particles change their positions with time. In a PSO system, particles fly around in a multidimensional search space. During flight, each particle adjusts its position according to its own experience, and the experience of neighboring particles, making use of the best position encountered by itself and its neighbors. When improved positions are being discovered these will then come to guide the movements of the swarm. The process is repeated and by doing so it is hoped, but not guaranteed, that a satisfactory solution will eventually be discovered [22].

The following is the conventional terminology of the variables in PSO: Let x and v denote a particle coordinates (position) and its corresponding flight speed (velocity) in a search space, respectively. Therefore, the $\boldsymbol{i}$th particle is represented as $x_i = [x_{i1}, x_{i2}, ..., x_{im}]$. Since $\boldsymbol{m}$ is the last dimension or coordinate of the position of the the $\boldsymbol{i}$th particle in the search space and so that $\boldsymbol{d} = 1, 2, ..., \ \boldsymbol{m}$.

The best previous position of the $\boldsymbol{i}$th particle is recorded and represented as [22],

$pbest_i = [pbest_{i1}, pbest_{i2}, ..., pbest_{im}]$.

The position of the best particle among all the particles in the group is represented by the *gbest*. In a particular dimension $\boldsymbol{d}$ there is a group best position which is $gbest_d$.

The velocity for the $\boldsymbol{i}$th particle is represented as, $v_i = [v_{i1}, v_{i2}, ..., v_{id}]$. The modified velocity and position of each particle can be calculated by using the following formulas:

$$v_{id}^{k+1} = w * v_{id}^{k} + c_1 * U * (pbest_{id}^{k} - x_{id}^{k}) + c_2 * U * (gbest_{d}^{k} - x_{id}^{k}) \tag{3.1}$$

$$x_{id}^{k+1} = x_{id}^{k} + v_{id}^{k+1} \tag{3.2}$$

$i = 1, 2, ..., n; \qquad d = 1, 2, ..., m$

Where

n number of particles in a group;

m number of members in a particle;

k pointer of iterations (generations);

w inertia weight factor;

c_1, c_2 acceleration factors;

U uniform random number in the range [0,1];

x_{id}^{k},v_{id}^{k} the position and velocity of the $\boldsymbol{i}$th particle in the $\boldsymbol{d}$th dimension at iteration k;

The search mechanism of the PSO using the modified velocity and position of individual based on (3.1) and (3.3) is illustrated in figure (3.1)

In the above procedures, the velocity should between $v_d^{min} \leq v_{id} \leq v_d^{max}$ If v_d^{max} is too high, particles might fly past good solutions. If v_d^{max} is too small, particles may not explore sufficiently beyond local solutions. In many experiences with PSO, was often set at 10 - 20% of the dynamic range of the variable on each dimension [22].

The constants c_1 and c_2 represent the weighting of the stochastic acceleration terms that pull each particle toward the *pbest* and *gbest* positions. Low values allow particles to move far from the target regions before being dragged back. On the other hand, high values

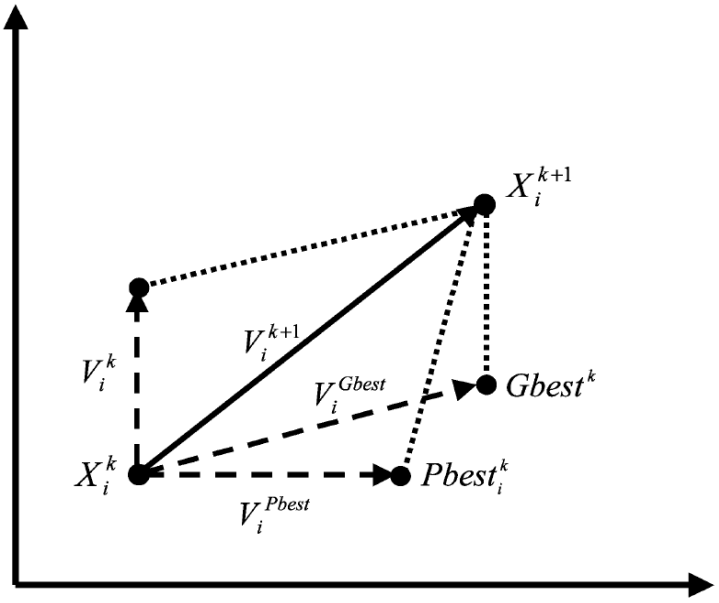

Figure 3.1: PSO search mechanism

result in sudden movement toward, or past, target regions. Hence, the acceleration constants c_1 and c_2 were often set to be 2 according to past experiences [22].

Suitable selection of inertia weight w in (3.1) provides a balance between global and local explorations, to find a sufficiently optimal solution. As originally developed w, often decreases linearly from about 0.9 to 0.4 during a run. In general, the inertia weight is set according to the following equation:

$$w = w_{max} - \frac{(w_{max} - w_{min})}{iter_{max}} \times iter \tag{3.3}$$

Where $iter_{max}$ is the maximum number of iterations (generations), and $iter$ is the current number of iterations.

3.3 FEATURES OF PSO

The main feauturs of the PSO algorithm are summarized as: simple concept, easy implementation, robustness to control parameters, and computational efficiency when compared with mathematical algorithm and other heuristic optimization techniques [7].

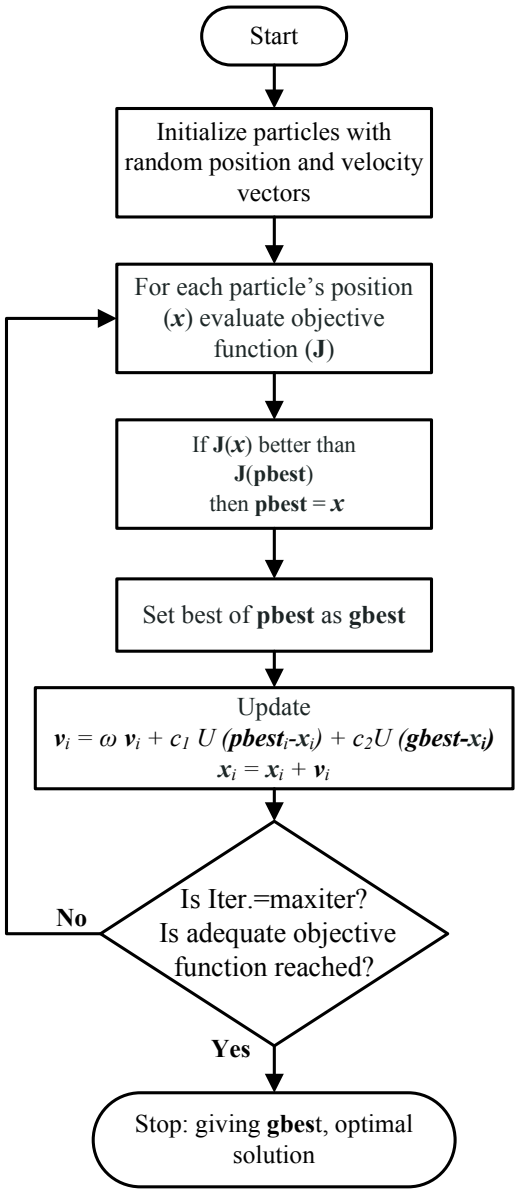

Figure 3.2: PSO algorithm flowchart

A PSO is considered as one of the most powerful methods for resolving the non-smooth global optimization problems. and has many key advantages as follows:

- PSO is a derivative-free technique just like as other heuristic optimization techniques.
- PSO is easy in its concept and coding implementation compared to other heuristic optimization techniques.

- PSO is less sensitivity to the nature of the objective function compared to the conventional mathematical approaches and other heuristic methods.
- PSO is less sensitivity to the nature of the objective function compared to the conventional mathematical approaches and other heuristic methods.
- PSO seems to be somewhat less dependent of a set of initial points compared to other evolutionary methods, implying that convergence algorithm is robust.
- PSO techniques can generate high-quality solutions within shorter calculation time and stable convergence characteristics than other stochastic methods.

The major drawback of PSO, like in other heuristic optimization techniques, is that it lacks somewhat a solid mathematical foundation for analysis to be overcome in the future development of relevant theories. Also, it can have some limitations for real-time ED (optimal economic dispatch) applications such as 5- minute dispatch considering network constraints since the PSO is also a variant of stochastic optimization techniques requiring relatively a longer computation time than mathematical approaches. However, it is believed that the PSO-based approach can be applied in the off-line real-world ED problems such as day-ahead electricity markets.

3.4 IMPLEMENTATION OF PSO FOR OPF PROBLEM

Although PSO has been used mainly to solve unconstrained, single-objective optimization problems, PSO algorithms have been developed to solve constrained problems, multi-objective optimization problems, and problems with dynamically changing landscapes.

Recently, PSO have been successfully applied to various fields of power system optimization such as power system stabilizer design, reactive power and voltage control, and dynamic security border identification [34].

Most of power system optimization problems including optimal power flow have complex and nonlinear characteristics with heavy equality and inequality constraints. The primary objective of the OPF problem is to determine the optimal combination of power outputs of all generating units so as to meet the required load demand at minimum operating cost while satisfying system equality and inequality constraints. Thus, over the past few years, in order to solve this problem, many modern methods have been developed and PSO is one of them.

The formulation of OPF for applying PSO is done by separating the problem variables to state variables, x, and control variables, u, as it was described in equations (2.14, 2.15, and 2.16), they also mentioned here as follows:

$$Min \quad J(\mathbf{x},\mathbf{u}) \tag{3.4}$$

subject to:

$$g(\mathbf{x},\mathbf{u}) = 0 \tag{3.5}$$

$$h(\mathbf{x},\mathbf{u}) \leq 0 \tag{3.6}$$

$$\mathbf{u} \in U \tag{3.7}$$

Where:

$$\mathbf{x} = [P_{G_1}, V_L, Q_G, S_{line}] \tag{3.8}$$

$$\mathbf{u} = [P_G, V_G, T, Q_C] \tag{3.9}$$

The equlity constraint in (3.5) are the nonlinear power flow equations as in (2.17 and 2.18)

The inequality constraints (3.6) are the functional operating constraints, such as transmission line limits, load bus voltage magnitude limits, generator reactive capabilities, and slack bus active power output limits. Constraints (3.7) define the feasibility region of the control variables of the problem such as the active power output limits of the generators (except the generator at the slack bus), generation bus voltage magnitude limits, transformer-tap setting limits, and bus shunt admittance limits.

Each particle in PSO is a vector containing the control variables $\mathbf{u}$, suggesting a possible solution to the OPF problem. Then the position of the $\boldsymbol{i}$th particle x_i can be represented as $x_i = \mathbf{u}_i = (u_{i1}, u_{i2}, ..., u_{im})$, where m is the number of dimensions and it is also represented the number of control variables, $d \in [1, m]$, $u_{id} \in [u_{id}^{min}, u_{id}^{max}]$.

u_{id}^{min}, and u_{id}^{max} are the lower and upper bounds of u_{id}. The particles are moving in an m dimensional space.

For consistency's sake, the general definition of the swarm particle is which used in the rest of the thesis, as in equations (3.1 and 3.3). Therefore, the $\boldsymbol{i}$th particle is represented as $x_i = [x_{i1}, x_{i2}, ..., x_{im}]$ instead of $\mathbf{u}_i$.

Each particle attempts to minimize the following objective function:

$$J_{aug} = \sum_{i=1}^{NG} F_i(P_{Gi}) + \lambda \left[\sum_{i=1}^{NS} \mu_i * h_i(\mathbf{x},\mathbf{u}) \right] \tag{3.10}$$

Since:

$$\mu_i = \begin{cases} 1; & h_i(\mathbf{x},\mathbf{u}) > 0 \\ 0; & h_i(\mathbf{x},\mathbf{u}) \leq 0 \end{cases} \tag{3.11}$$

Here the objective function becomes unconstrained or augmented objective function by using the classical penalty functions principle. All inequality constraints in equation (3.6) replaced by penalty terms. While the power balance equations (3.5), which are the equality constraints, is solved for each particle and in every iteration by Newton-Raphson power flow algorithm, therefore no need to use a penalty function for this equality constraint in equation (3.10).

J_{arg} is the penalized objective function and $F_i(P_{Gi})$ is the cost of the real power from the generator P_{Gi} while λ is the penalty factor for operating constraints. μ_i is an indicator of occurring any violations and work outside the feasibility region of the solution. It has only two values as in equation (3.11), they are 1 when a violation of the limits occurred in the corresponding constraint and 0 when there is no violation. The penalty terms that have been used are quadratic penalty functions as those in equation (2.28). Whereas NG is the

number or generators while NS is the number of the state variables to be bounded within their limits. The penalty factor λ is used to penalize the fuel cost proportional to the amount of constraint violations, the suitable value of the penalty factor is chosen after some runs of the algorithm [35]. According to the equations (3.1 and 3.3) in every iteration each particle of the swarm updates its position coordinates (dimensions) until the termination condition of the algorithm is met.

CHAPTER 4

STUDY CASES AND SIMULATION RESULTS

4.1 IEEE 30-BUS TEST SYSTEM

It is instructive to apply the PSO algorithm to solve OPF for IEEE 30-Bus Test System.

4.1.1 The Data of The System

The system is shown in figure (4.1) and the data of the buses, lines, and generators are given in Appendix (A). It consists of six conventional thermal generators at buses 1, 2, 5, 8, 11, and 13, and 41 branches, four of them are transformers with off-nominal tap ratios in branches 6-9, 6-10, 4-12, and 28-27. In addition, the buses 10, 12, 15, 17, 20, 21, 23, 24, and 29 are equipped with shunt VAR compensators. The limits of control variables are indicated in table (4.1). For the other operating (state) variables such as voltages at load buses, the limits are [0.95-1.1]. The limits of reactive power of generators Q_G and the transmission lines ratings are both indicated in generator data and line data tables respectively in Appendix (A).

Table 4.1: Control variables and their limits

The control variable	P_{G1} (MW)	P_{G2} (MW)	P_{G3} (MW)	P_{G4} (MW)	P_{G5} (MW)	P_{G6} (MW)	V_{Gs} (pu)	T_s	Q_{shs} (MVAR)
The upper limit	200	80	50	35	30	40	0.95	0.9	0
The lower limit	50	20	15	10	10	12	1.1	1.1	5
Ts: transformer tap ratio; VGs: voltage at generator bus; Qsh: VAR compensation.									

4.1.2 The PSO Algorithm and Its Parameters for Solving OPF

The skeleton of PSO algorithm is taken form these references [36, 37] after it has been modified for solving OPF. Matlab is used for running the algorithm. Initially several runs

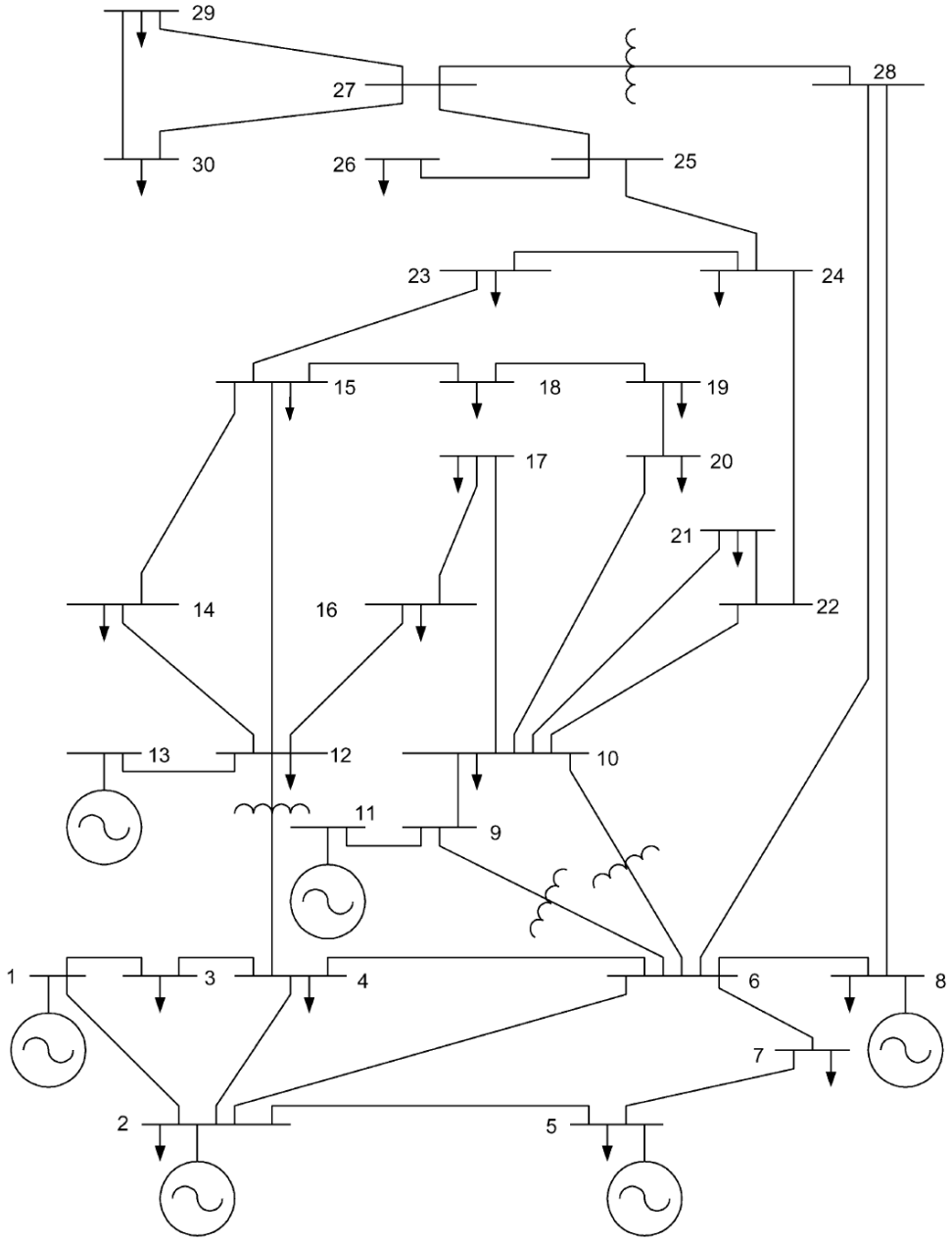

Figure 4.1: Single-line diagram of IEEE 30-bus test system [20]

are done besides to valuable information in [20, 21, 22] to select the suitable parameters for PSO algorithm. The inertia weight is decreasing linearly with iterations with its initial value at 0.9 and ultimate value at 0.4, while the acceleration factors C_1 and C_2 are equal to 2 and the number of particles is 10. The termination condition is when the 5 significant

digits after the decimal point of the optimal solution have not changed for last 50 iterations, the algorithm will then consider this as an optimal solution. In addition, the maximum number of iterations after which the algorithm also terminates is 500.

4.1.3 The Objective Function

The objective function is to minimize the operating (fuel) cost of the system as in equation (3.10) which is used in PSO algorithm. For convenience, the equation (3.10) are rewritten again as following:

$$J_{aug} = \sum_{i=1}^{NG} F_i(P_{Gi}) + \lambda \left[\sum_{i=1}^{NS} \mu_i * h_i(\mathbf{x},\mathbf{u}) \right] \tag{3.10}$$

Since:

$$\mu_i = \begin{cases} 1; & h_i(\mathbf{x},\mathbf{u}) > 0 \\ 0; & h_i(\mathbf{x},\mathbf{u}) \leq 0 \end{cases} \tag{3.11}$$

Where μ_i is an indicator of occurring any violations in the constraints. It has only two values, 1 when a violation of the limits occurred of the corresponding constraint and 0 when there is no violation.

The penalty functions are quadratic penalty functions as those in equation (2.28) which is as:

$$J_{aug} = J + \lambda_P (P_{G_1} - P_{G_1}^{lim})^2 + \lambda_V \sum_{i=1}^{NL} (V_{L_i} - V_{L_i}^{lim})^2 + \lambda_Q \sum_{i=1}^{NG} (Q_{G_i} - Q_{G_i}^{lim})^2 + \lambda_S \sum_{i=1}^{nl} (S_{line_i} - S_{line_i}^{max})^2 \tag{2.28}$$

Where x^{lim} is the limit value of the state variable x given as:

$$x^{lim} = \begin{cases} x^{max}; & (x > x^{max}) \\ x^{min}; & (x < x^{min}) \end{cases} \tag{2.29}$$

Whereas $\lambda_P = \lambda_V = \lambda_Q = \lambda_S = \lambda$.

After some trial runs of PSO algorithm, the penalty factor (λ) has been chosen to be 100000.

4.1.4 Study of Base Case

The load flow of the initial operating point which is given in bus data table in Appendix (A), illustrates that there are violations in the lower limit of voltage at load buses 18, 19, 20, 21, 22, 23, 24, 25, 26, 27, 29, 30. Notice there is no violation for bus 28 although it is also far from generators, that because this bus is fed by two branches and one of them directly from generator at bus 8. Furthermore, there is a rating violation of the transmission line which connects the buses 1 and 2.

However, by using PSO algorithm with all of control variables (i.e. P_{Gs}, V_{Gs}, T_s, and Q_{shs}) for solving the OPF of the base case ($283.4MW$). Then the violations can be alleviated as it is shown in figure (4.2). Moreover, the cost of the real output power of generators is also minimized to 798.43 $\$/hr$ as it is illustrated in table (4.2) and figure (4.3).

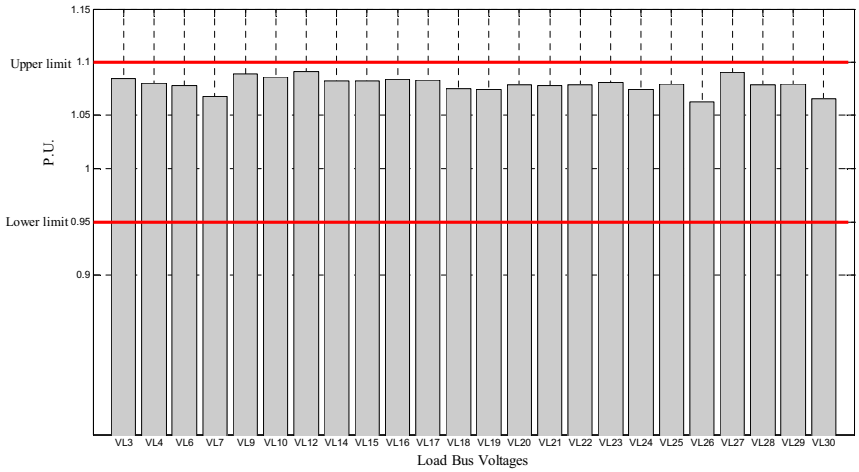

Figure 4.2: Voltage levels at load buses of base case of IEEE 30-bus test system

Table 4.2: Generators outputs of base case ($283.4\ MW$)

P_{G1} (MW)	P_{G2} (MW)	P_{G3} (MW)	P_{G4} (MW)	P_{G5} (MW)	P_{G6} (MW)	Losses (MW)	Cost ($/hr)
176.94	48.71	21.27	21.09	11.83	12.00	8.4382	798.43

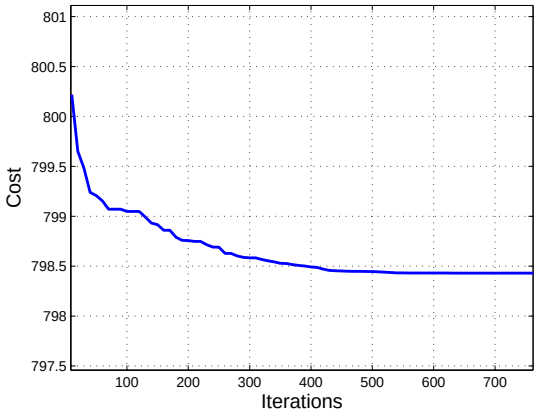

Figure 4.3: Cost vs. iterations with all control variables of base case

4.1.5 Application of Sensitivity Analysis for OPF

Now, the sensitivity analysis of optimal power flow is applied for the base case to see which combination of control variables could adjust the violations before the OPF of the base case. From the procedures of finding sensitivity matrices of voltage and current as it discussed in Appendices (C.3 and C.4), the resulting order of state and control variables in addition to the visualized sparsity pattern of elements in matrices Su and R are shown in figure (4.4) and figure (4.5) respectively.

Table (4.3) presents the most effective or dominant control variables for every violated bus voltage are ordered from up to down. This order of control variables have been accomplished by Singular Value Decomposition (SVD) between the voltage sensitivity matrix S_u and its corresponding column vectors of state and control variables, for more information about SVD refer to [38].

Therefor, the selection of control variables becomes more effective to satisfy the constraints. As it is shown in figure (4.5), the control variables for every line flows are four, the voltage magnitudes and phase-angles at both ends of the line. For the rating constraint of the transmission line 1-2, the control variables are voltage magnitudes and phase-angles of both bus 1 and bus 2. Fortunately, the magnitude of V_1 and V_2 are control variables,

The sensitivity analysis of voltages				
Δx			$\mathbf{Su=-Jx^{-1}Ju}$	Δu
Pg1	d14	V6	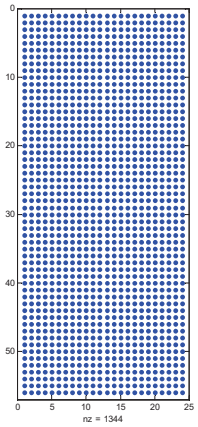	Pg2
Qg1	d15	V7		Pg5
Qg2	d16	V14		Pg8
Qg5	d17	V15		Pg11
Qg8	d18	V16		Pg13
Qg11	d19	V17		Vg1
Qg13	d20	V18		Vg2
d2	d21	V19		Vg5
d3	d22	V20		Vg8
d4	d23	V21		Vg11
d5	d24	V22		Vg13
d6	d25	V23		T9
d7	d26	V24		T10
d8	d27	V25		T12
d9	d28	V26		T27
d10	d29	V28		Qsh10
d11	d30	V29		Qsh12
d12	V3	V30		Qsh15
d13	V4			Qsh17
				Qsh20
				Qsh21
				Qsh23
				Qsh24
				Qsh29
Where **d** stands for phase-angle of bus voltage (δ).				

Figure 4.4: Voltage sensitivity matrix S_u and its state Δx and control Δu variables

The sensitivity analysis of Currents			
Δx		$\mathbf{R=-Jx^{-1}Ju}$	Δu
I1_2	I16_17	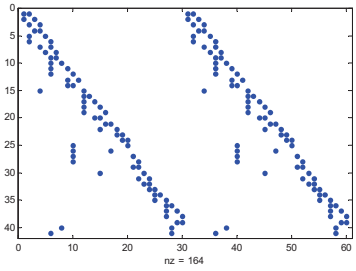	V1
I1_3	I15_18		.
I2_4	I18_19		.
I3_4	I19_20		.
I2_5	I10_20		.
I2_6	I10_17		.
I4_6	I10_21		.
I5_7	I10_22		.
I6_7	I21_22		V30
I6_8	I15_23		d1
I6_9	I22_24		.
I6_10	I23_24		.
I9_11	I24_25		.
I9_10	I25_26		.
I4_12	I25_27		.
I12_13	I28_27		.
I12_14	I27_29		.
I12_15	I27_30		.
I12_16	I29_30		.
I14_15	I8_28		d30
	I6_28		
Where $\mathbf{I_{1\text{-}2}}$ stands for the power flow in the branch (1-2).			

Figure 4.5: Current sensitivity matrix R and its state Δx and control Δu variables

while the phase-angles have a strong relationship with real power flows, these latter are also controllable through this branch.

The sensitivity analysis is useful, especially in reducing the problem dimension of large systems with many buses and that of course means many control variables as well. When control variables increase the dimensions of the particles in PSO algorithm also increase and that can cause a complexity for manipulating the dimensions of the particles [21].

Table 4.3: Ordered control variables for violated voltages of load buses

VL19	VL20	VL21	VL22	VL23	VL24	VL25	VL26	VL27	VL29	VL30
V8	T27	V2	T27	V1	V8	V1	V8	T27	V8	V8
V2	V5	V8	V1	V2	V5	V5	V2	V13	V1	V1
V1	V8	V1	V2	V8	V2	V2	V5	T12	V2	V2
V5	V2	V5	V5	V5	V1	V13	V1	Qsh23	V5	V5
V11	V1	T27	V8	T27	V11	T12	V13	Qsh29	V13	V13
T9	V11	V11	V13	Qsh29	T9	V8	T12	Qsh24	T12	T12
T27	T9	T9	T12	V11	T27	V11	T10	V1	Qsh23	V11
V13	V13	V13	V11	T9	T10	T9	V11	V2	V11	T9
T12	T12	T12	T9	V13	V13	T10	T9	V8	T9	T10
Qsh23	T10	Qsh29	Qsh29	T12	T12	Qsh20	Qsh15	V5	T10	Qsh15
Qsh29	Qsh29	Qsh23	Qsh23	T10	Qsh15	Qsh15	Qsh23	T10	Qsh15	T27
T10	Qsh24	T10	T10	Qsh20	Qsh17	T27	T27	Qsh15	T27	Qsh29
Qsh24	Qsh23	Qsh15	Qsh15	Qsh21	Qsh20	Qsh12	Qsh12	V11	Qsh24	Qsh12
Qsh12	Qsh17	Qsh12	Qsh12	Qsh17	Qsh29	Qsh17	Qsh17	T9	Qsh12	Qsh23
Qsh15	Qsh21	Qsh20	Qsh24	Qsh12	Qsh12	Qsh23	Qsh20	Qsh12	Qsh17	Qsh24
Qsh20	Qsh10	Qsh17	Qsh21	Qsh10	Qsh23	Qsh29	Qsh24	Qsh20	Qsh20	Qsh20
Qsh17	Qsh12	Qsh24	Qsh20	Qsh24	Qsh10	Qsh24	Qsh21	Qsh17	Qsh29	Qsh17
Qsh21	Qsh20	Qsh10	Qsh17	Qsh15	Qsh21	Qsh21	Qsh29	Qsh21	Qsh21	Qsh21
Qsh10	Qsh15	Qsh21	Qsh10	Qsh23	Qsh24	Qsh10	Qsh10	Qsh10	Qsh10	Qsh10

Therefor, finding and using the most effective control variables to adjust and correct the violations can decrease the dimensions in PSO and enhance its performance.

4.1.6 PSO Solution for Base Case

Now let's using the most effective control variables to adjust violations in initial operating point of IEEE 30-bus test system. Several desired combinations of dominant control variables (as they are ordered in table (4.3)) are selected, some of them are sufficient combination of most effective control variables to bring back the violations in the voltage of load buses within their limits in base case 283.4 MW. Combinations of most effective control variables and the result of PSO for each combinations are listed in table (4.4). As it is shown in table (4.4) except using all control variables, the most effective control variables combination of P_{gs} and V_{gs} is the best with cost 799.86 $\$/hr$. While for other less number of control variables in addition to P_{gs}, the combination of most effective control variables of $P_{gs}, V_{g1}, V_{g2}, V_{g5}$ and V_{g8} and the other of $P_{gs}, V_{g1}, V_{g2}, V_{g8}$ and T_{27} are succeeded to adjust

Table 4.4: PSO result of combinations of most effective control variables for base case

Case	Violation	Control variables	Still exist violations	Cost
283.4MW	*V_L18…30, S_{line1}	(**P_{gs}), (Vg1, Vg5, Vg8)	V_{L26}, V_{L30}, S_{line10}	818.92
283.4MW	V_L18…30, S_{line1}	(P_{gs}), (Vg1, Vg2, Vg8)	V_{L30}, S_{line10}	805.51
283.4MW	V_L18…30, S_{line1}	(P_{gs}), (Vg1, Vg2, Vg5, Vg8, Vg13)	V_{L30}	800.17
283.4MW	V_L18…30, S_{line1}	(P_{gs}), (Vg1, Vg2, Vg8), (T27)	-----	802.41
283.4MW	V_L18…30, S_{line1}	(P_{gs}), (Vg1, Vg2, Vg5, Vg8)	-----	800.22
283.4MW	V_L18…30, S_{line1}	(P_{gs}), (Vgs)	-----	799.86
283.4MW	V_L18…30, S_{line1}	All (i.e. Pgs, Vgs, Ts, Qshs)	-----	798.43

* V_L18…30 stands for violations at buses 18, 19, 20, 21, 22, 23, 24, 25, 26, 27, 29, 30.
** P_{gs} stands for all real power of generators except the first generator at slack bus.

all violations, but the former combination produces lower cost 800.22 $\$/hr$.

4.1.7 PSO Solution for Different Loading

For IEEE 30-bus test system with other cases of loading, PSO has been applied with using most effective control variables to adjust the violations, if they exist. The results are shown in table (4.5).

Table 4.5: PSO result for several loading cases of IEEE 30-bus test system

Total loading	Violation	Control variables	Cost
125MW	----	(*P_{gs})	309.060
150MW	V_L30	(P_{gs}), Vg1, Vg2, Vg8	374.577
200MW	V_L26, V_L29, V_L30	(P_{gs}), Vg1, Vg2, Vg5, Vg8	517.827
250MW	----	(P_{gs})	681.602
275MW	S_{line1}	(P_{gs}), Vg1, Vg2	769.947
300MW	S_{line1}	(P_{gs}), Vg1, Vg2	861.65
325MW	V_L26, V_L30, S_{line1}	(P_{gs}), Vg1, Vg2, Vg5, Vg8, Vg13	956.922
350MW	V_L26, V_L29, V_L30, S_{line1}	(P_{gs}), Vg1, Vg2, Vg5, Vg8, Vg11, Vg13, T9, T10, T12, Qsh15	1058.605

* P_{gs} stands for Pg_2, Pg_5, Pg_8, Pg_{11} and Pg_{13}.

Notice: Every OPF solution of the previous loading case is considered as an initial operating point for the following loading case. for example, if the OPF of the loading case 125 MW has been solved then the OPF of the successive loading case 150 MW considers

the solution of the previous loading case 125 MW as its initial point and so on.

V_{L26}, V_{L29}, and V_{L30} are the weakest buses in the system that are susceptible to violations more than other buses. While the transmission line that connect bus 1 and bus 2 is the weakest transmission line and it has suffered from violation of its rating for several loading cases. In the last case 350 MW a variety of control variables are needed to keep the system in secure operation.

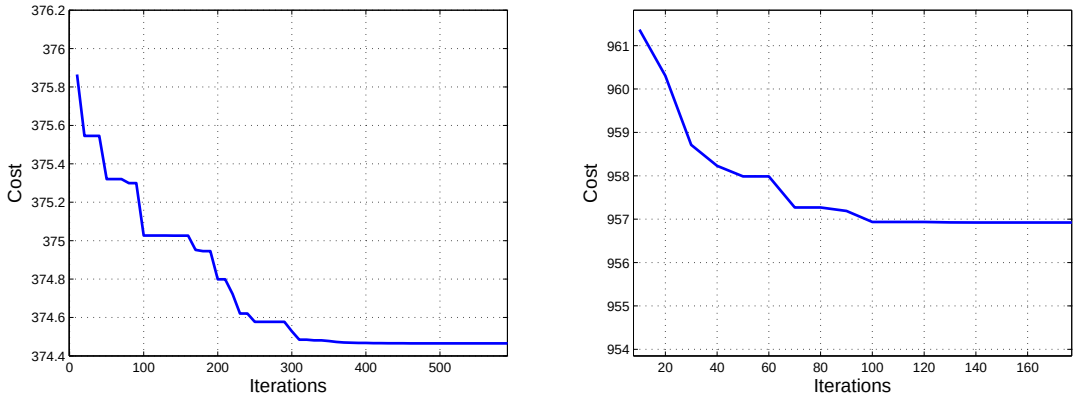

(a) 150 MW (b) 325 MW

Figure 4.6: Cost vs. iterations of two loading cases

4.2 6-BUS SYSTEM INCLUDING WIND-POWERED GENERATORS

For analysis and investigation aim, it could be better to present the implementation of PSO to solve OPF for a relatively small system when the wind power is considered, especially for a used model in equation (1.10) with an objective function that contains integrations, is used.

4.2.1 The Data of The System

The 6-Bus System in figure (4.7) has been adopted for study of optimal dispatch including wind power. This system consists of six buses and four generators at buses 1, 2, 3, and 4, generators at buses 3 and 4 are wind-powered generators. There are seven

transmission lines, and there are no LTC transformers or VAR compensation devices in this system. Bus data, line data and generators data are all in Appendix (B).

The higher output of each wind-powered generator is 40 MW. While the direct cost of wind power (6 and 8 \$/($MW.hr$)) for wind-powered generator 3 and 4 respectively. The difference in direct cost of wind power is for variety purpose, to get more options of dispatching.

The parameters of the wind turbine are cut-in wind speed $v_i = 5m/s$, rated wind speed $v_r = 15m/s$, and cut-out wind speed $v_o = 45m/s$.

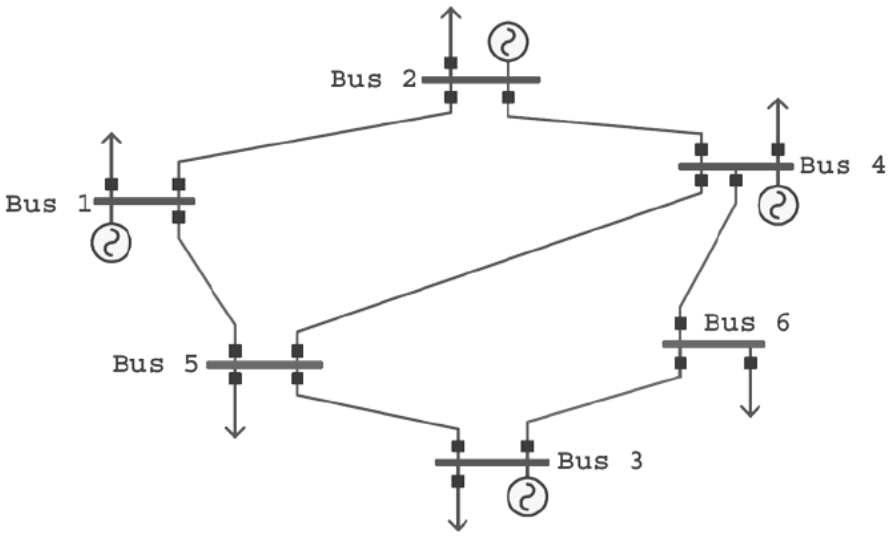

Figure 4.7: Single-line diagram of 6-bus system [39]

4.2.2 The Objective Function

Implementing PSO algorithm with a model discussed in section (1.2), which includes the wind power direct cost and penalty costs of underestimation and overestimation of wind power. The objective function as in equation (1.10) is:

$$J = \sum_{i=1}^{M} C_i(p_i) + \sum_{i=1}^{N} C_{w,i}(w_i) + \sum_{i=1}^{N} C_{p,i}(w_i) + \sum_{i=1}^{N} C_{r,i}(w_i) \tag{1.10}$$

Where:

$\sum_{i=1}^{M} C_i(p_i)$ is the cost of the real power of thermal-generators, $\sum_{i=1}^{N} C_{w,i}(w_i)$ is the

direct cost of wind power, $\sum_{i=1}^{N} C_{p,i}(w_i)$ is the penalty cost of the underestimation of the available wind power, and $\sum_{i=1}^{N} C_{r,i}(w_i)$ is the reserve cost of the overestimation of the available wind power. The two latter terms in the objective functions need integration as they are shown in equations (1.3 and 1.4), which are:

$$C_{p,i} = k_{p,i} \int_{w_i}^{w_{r,i}} (w - w_i) f_w(w) dw \tag{1.3}$$

$$C_{r,i} = k_{r,i} \int_{0}^{w_i} (w_i - w) f_w(w) dw \tag{1.4}$$

Figure (4.8) illustrates the cumulative probability distribution of wind power, it has been produced from the integration of equation (2.13). This figure is important for the following investigations.

Note: w is the available wind power while w_r is for rated wind power.

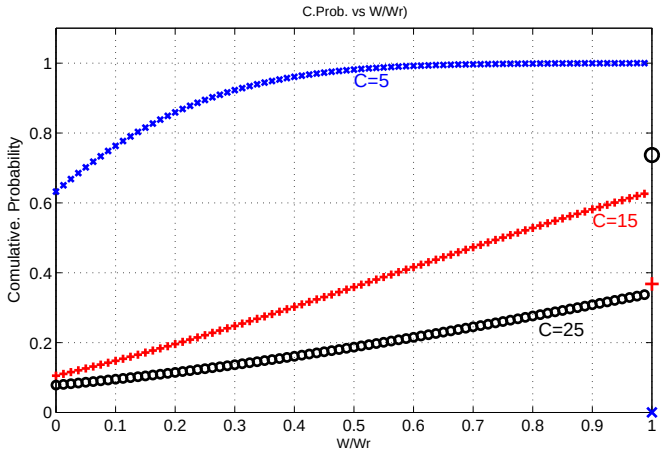

Figure 4.8: Cumulative probability distribution of wind power vs. normalized wind power

4.2.3 PSO Solution for Base Case

The table (B.1) in Appendix (B) is the base case with total load of 400 MW.

The parameters of Weibull distribution of wind speed here are scale factor c =5 m/s, while the shape factor k is 2. The reserve cost coefficient as a result of overestimation of available wind power is 1 $\$/MW.hr$. On the other hand, penalty cost coefficient as a result

of underestimation of available wind power is 0 $\$/MW.hr$, this means the utility owns wind turbines so there is no penalty of surplus produced wind power. The changing of these coefficients and their effect on the total cost will be investigated later.

The result of the base case by using PSO algorithm is in table (4.6), there is no violations in voltage at load buses for the base case. The minimum cost of real power form both thermal and wind power is 4777.49 $\$/hr$. Wind-powered generators in these conditions supply maximum outputs because they are more economic. While the first thermal generator supplies less power to the system than the second generator because its generated power is more expensive.

As it is shown in table (4.6) the outputs of generators equal to the demand plus losses in the system.

Table 4.6: PSO result for base case ($400MW$) of 6-bus system

P_{G1} (MW)	P_{G2} (MW)	P_{G3} (MW)	P_{G4} (MW)	Losses (MW)	Cost ($/hr)
92.82	230.64	40	40	3.462	4777.49
C =5 m/s, K=2. (Weibull PDF parameters) Kr=1 $/MW.hr, Kp=0 $/MW.hr as utility owns wind turbines (wind power cost factors).					

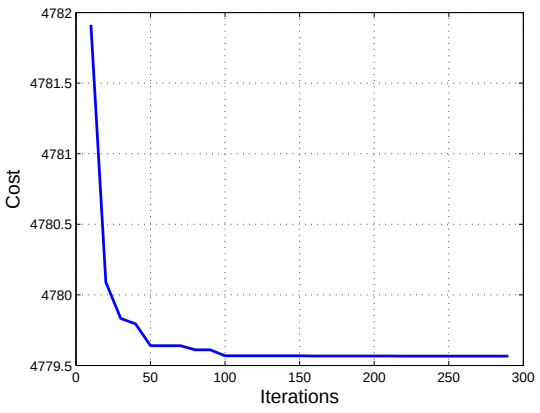

Figure 4.9: Cost vs. iterations of 400 MW case of 6-bus system

4.2.4 PSO Solution for Different Loading

The OPF solution by PSO algorithm when the system load increases gradually is as in table (4.7).

Table 4.7: PSO result for OPF of different load cases of 6-bus system

Load (MW)	$\mathbf{P_{G1}}$ (MW)	$\mathbf{P_{G2}}$ (MW)	$\mathbf{P_{G3}}$ (MW)	$\mathbf{P_{G4}}$ (MW)	**Losses** (MW)	**Cost** ($/hr)
400	92.82	230.64	40	40	3.46	4777.49
450	125.10	250	40	40	5.10	5524.48
500	177.05	250	40	40	7.05	6336.25
C =5 m/s, K=2. (Weibull PDF parameters) K_r=1 $/MW.hr, K_p=0 $/MW.hr.						

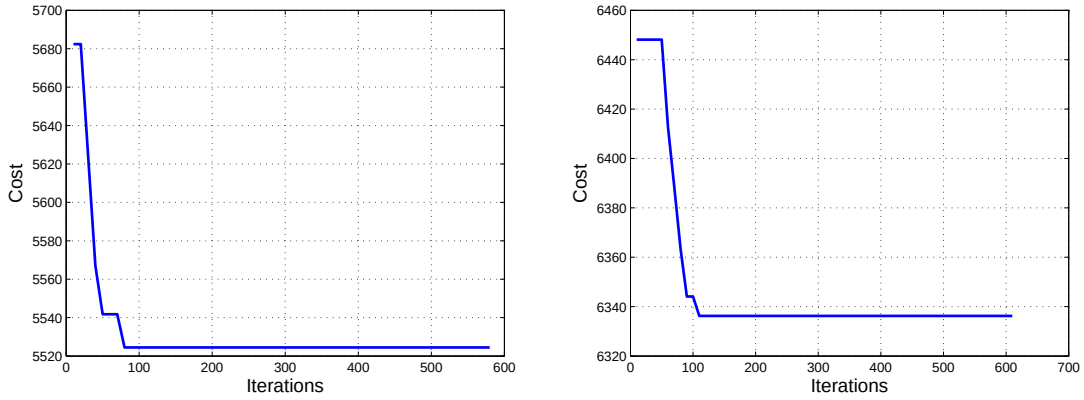

(a) 450 MW (b) 500 MW

Figure 4.10: Cost vs. iterations of two load cases

Whereas the economic dispatch result is in table (4.8). This result without considering the limits of state variables such as load bus voltages or ratings of transmission lines since there are no violations in the system. In addition, the losses also is ignored because they are relatively low.

There is a small difference of the scheduling of generators' outputs in results of OPF and economic dispatch (ED) as shown in tables (4.7) and (4.8).

Table 4.8: PSO result for ED of different load cases of 6-bus system

Load (MW)	P_{G1} (MW)	P_{G2} (MW)	P_{G3} (MW)	P_{G4} (MW)	Cost ($/hr)
400	86.66	233.34	40	40	4728.225
450	120	250	40	40	5448.225
500	170	250	40	40	6222.225
C =5 m/s, K=2. (Weibull PDF parameters) K_r=1 $/MW.hr, K_p=0 $/MW.hr.					

4.3 THE EFFECTS OF WIND POWER COST COEFFICIENTS

Next variety of wind power cost coefficients and wind speed factors will be investigated. So that their effects on the output schedule of the generators and hence the total cost in the base case 400 MW are presented as following:

The shape factor of wind speed probability distribution $k = 2$ and it is kept constant at this value. While the scale factor c is changing between $5m/s$ to 25 m/s. The constant direct costs of wind power from wind-powered generators 3 and 4 are 6 and 8 $\$/(MW.hr)$ respectively. For sake of convenience, hereinafter the units will be dropped from these coefficients.

4.3.1 The Effects of Reserve Cost Coefficient

First, assume that the utility owns wind turbines ($k_p = 0$) so that the penalty cost of additional available wind power over scheduled power will be 0 as it derived from equation (1.3).

Figure (4.11) shows the result of PSO algorithm for the outputs of generators as a function of the scale factor of Weibull distribution of wind speed c for different values of reserve cost coefficient k_r. When c scale factor of Weibull distribution of wind speed increases, the reserve cost decreases. That can be verified from figure (4.8). When c increases, the probability of wind power decreases, then the reserve cost reduces as well. Since the reserve cost reduces by increasing c, the outputs of wind-powered generators will increase as in figure (4.11b). In figure (4.11c) there is a small increase in wind-powered

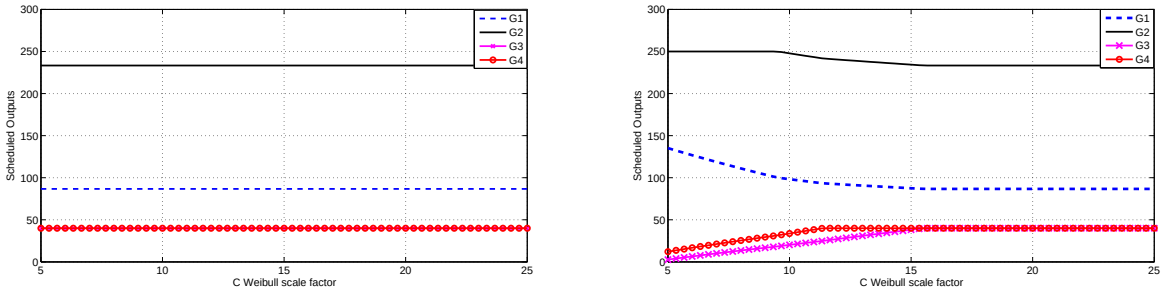

(a) k_r=1 (b) k_r=10

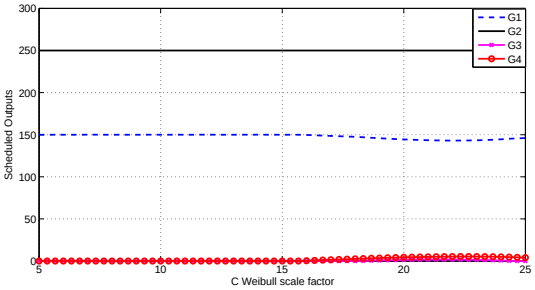

(c) k_r=100

Figure 4.11: Generator outputs vs. Weibull scale factor (c) for some values of reserve cost in base case 400 MW

generators form c =20 to c =25, it is a small change because the reserve cost coefficient in this case relatively high k_r=100.

Critical Reserve Cost Coefficient:

Figure (4.12) shows outputs of generators for a variation of reserve cost coefficient k_r for two values of scale factor $c = 5$ and $c = 20$ in order to see where the critical change in wind power schedule begins. In figure (4.12a) when c=5, the critical change in wind power schedule starts when $k_r = 6$ for generator (3) and $k_r = 8.6$ for generator (4), the change happens in generators (3) before generator (4) because generator (3) has a higher direct cost (8 \$/$MW.hr$) than that of (4) generator (6 \$/$MW.hr$). While in the other case when c=20 as in figure (4.12b), the change of wind power scheduling occurs at higher values of k_r

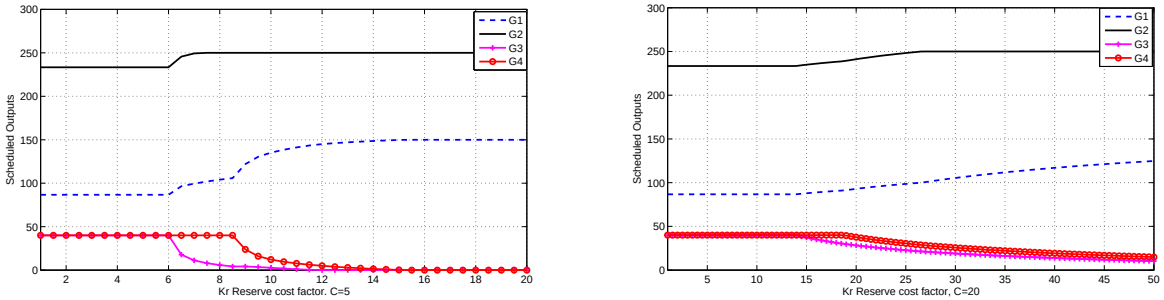

(a) c=5 (b) c=20

Figure 4.12: Generator outputs vs. reserve cost coefficient (k_r) for two values of scale factor (c) in base case 400 MW

because the high value of scale factor c of Weibull distribution of wind speed .

4.3.2 The Effects of Penalty Cost Coefficient

When $k_r = 0$ and $k_p \neq 0$, the schedule of generators as in figure (4.13a) for various values of k_p remains constant for different values of scale factor c. In this case it should get

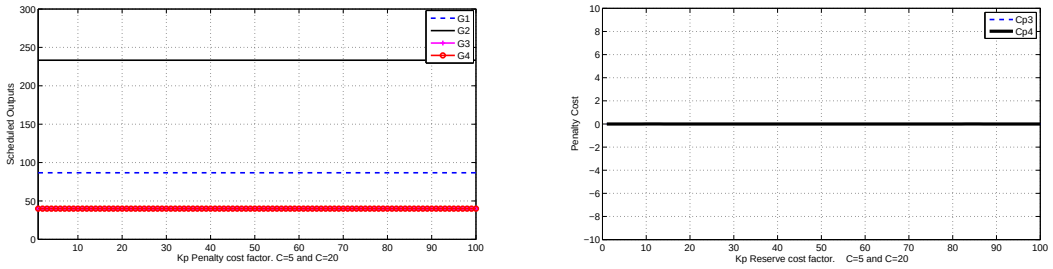

(a) Generators' Outputs (b) Penalty Cost C_p

Figure 4.13: Generators' outputs and penalty cost C_p vs. penalty cost coefficient k_p for two values of scale factor c in base case 400MW

all available wind power since there is a penalty cost for a surplus wind power. Figure (4.13b) shows that C_p=0 because all available wind power has been scheduled from both

wind-powered generators.

4.3.3 The Effects of The Reserve and Penalty Cost Coefficients

The effect of both of the reserve and the penalty cost coefficients when they are not zero ($k_r \neq 0$ and $k_p \neq 0$) is illustrated in figure (4.14)

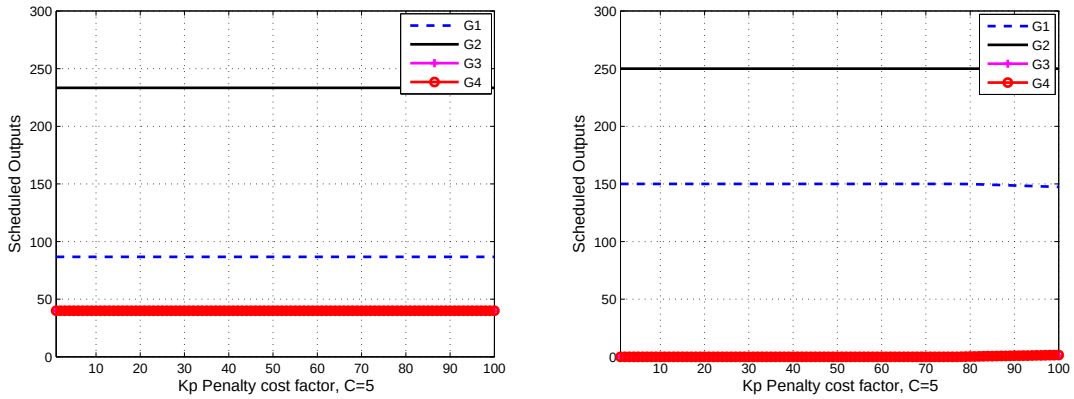

(a) $k_r = 0$ (b) $k_r = 60$

Figure 4.14: Generators' outputs vs. penalty cost coefficient k_p for some values of reserve cost coefficient k_r in the base case $400MW$ and $c = 5m/s$

When the reserve cost coefficient k_r increases, the scheduled wind power decreases. Until no scheduled power comes from wind-powered units when $k_r \geq 60$; because the high value of k_r makes the wind power to be not an economic option. Then all the scheduled power comes from thermal-powered units for any value of k_p, as in figure (4.14b).

Figure (4.15) can be considered as a part of figure (4.14) when kr=20 but now for two higher values of the scale factor c=10 and c=20.

As it is shown in figure (4.15), with a higher scale factor c of the probability distribution of wind speed, the outputs of wind-powered generators become higher as well. Furthermore, figure (4.15a) illustrates that the wind power outputs will increase with higher values of the penalty cost coefficient k_p.

This is what happens when the utility does not own the wind turbine, therefore the

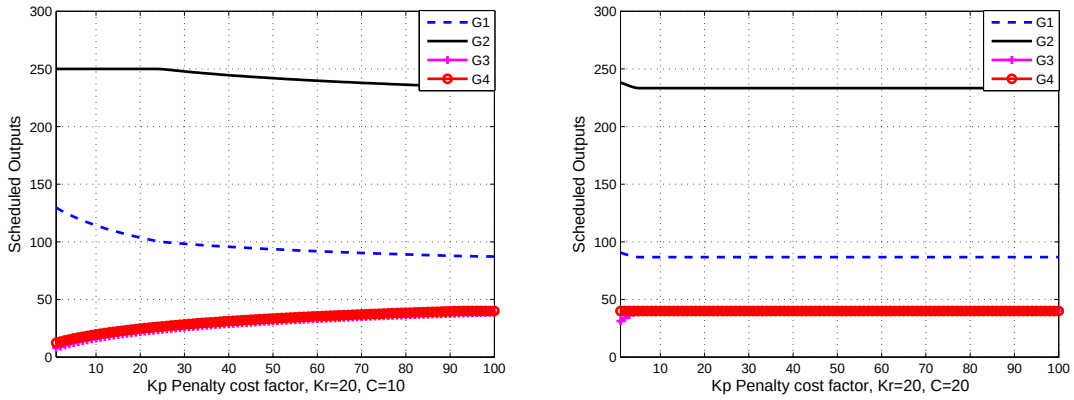

(a) $c = 10$ (b) $c = 20$

Figure 4.15: Generators' outputs vs. penalty cost coefficient k_p for two values of scale factor c when k_r=20

scheduled wind power is produced as a compromise between the penalty cost and the reserve cost of wind power.

CHAPTER 5

CONCLUSION AND FURTHER WORK

5.1 CONCLUSION

The implementation of PSO algorithm to solve the OPF problem is useful and worth of investigation. Moreover, PSO algorithm is easy to apply and simple since it has fewer number of parameters to deal with comparing to other modern optimization algorithms. In addition, PSO algorithm is appropriate for optimal dispatch of real power of generators that include wind-powered generators.

The used model of real power optimal dispatch for systems that include wind power uses the probabilities of underestimation and overestimation of available wind power. It also takes into account whether the utility owns wind turbines or not; these are the main features of this model. Furthermore, the probability manipulation of wind speed and wind power of the model is suitable since wind speed itself is difficult to predict and hence the wind power as well.

In IEEE 30-bus test system, OPF has been solved by using PSO and giving the minimum cost for several load cases. At the same test system applying OPF sensitivity analysis can give an indication to which of control variables have most effect to adjust violations of operating constraints.

The variations of wind speed parameters and their impacts on total cost investigated by 6-bus system, some valuable conclusion have been noticed.

5.2 FURTHER WORK

PSO algorithm needs some work on selecting proper parameters and it also needs some further mathematical description for its convergence. PSO can be applied in wind power bid marketing between electric power operators.

The used model can be adopted for larger power systems with wind power. In addition

to operating cost, the environment effects and security or risk of wind power penetration can be included in the used model and it becomes multi-objective model of optimal dispatch.

Fuzzy logic is worth of investigation to be used instead probability concept which is used here, especially when security of wind power penetration is included in the model.

Using most effective control variables to adjust violations in OPF needs more study since this concept could be applied for large systems and it can be helpful, especially along side the implementation of PSO algorithm.

The incremental reserve and penalty costs of available wind power can be compared to incremental cost of conventional-thermal units that have a quadratic cost; this comparison could lead to useful simplifications of an economic dispatch model that includes thermal and wind power.

REFERENCES

[1] C.-L. Chen, "Optimal wind–thermal generating unit commitment," vol. 23, no. 1, pp. 273–280, 2008.

[2] R. Thresher, M. Robinson, and P. Veers, "To capture the wind," vol. 5, no. 6, pp. 34–46, 2007.

[3] Global Wind Energy Council (GWEC), "Global wind statistics 2011," February 2012.

[4] Global Wind Energy Council (GWEC), "Wind energy makes sound economic sense," March 2012.

[5] P. Morthorst. and S. Awerbuch, "The economics of wind energy, a report by the european wind energy association," March 2009.

[6] R. A. Jabr and B. C. Pal, "Intermittent wind generation in optimal power flow dispatching," *IET Generation, Transmission & Distribution*, vol. 3, no. 1, pp. 66–74, 2009.

[7] K. Y. Lee and J.-B. Park, "Application of particle swarm optimization to economic dispatch problem: Advantages and disadvantages," in *Proc. IEEE PES Power Systems Conf. and Exposition PSCE '06*, pp. 188–192, 2006.

[8] M. R. AlRashidi and M. E. El-Hawary, "A survey of particle swarm optimization applications in electric power systems," vol. 13, no. 4, pp. 913–918, 2009.

[9] X. Wei, Y. Liu, and D. Zhao, "Review of dynamic dispatch research considering intermittent power generation," in *Proc. Asia-Pacific Power and Energy Engineering Conf. (APPEEC)*, pp. 1–5, 2011.

[10] M. S. S. J. Duncan Glover and T. Overbye, *Power System Analysis and Design*. New delhi: CL-Engineering, 4th ed., 2008.

[11] A. J. Wood and B. F. Wollenberg, *Power Generation, Operation and Control*. New York: Wiley, 2nd ed., 1996.

[12] J. Hetzer, D. C. Yu, and K. Bhattarai, "An economic dispatch model incorporating

wind power," vol. 23, no. 2, pp. 603–611, 2008.

[13] L. Wang and C. Singh, "Pso-based multi-criteria economic dispatch considering wind power penetration subject to dispatcher's attitude," in *Proc. 38th North American Power Symp. NAPS 2006*, pp. 269–276, 2006.

[14] X. Liu and W. Xu, "Minimum emission dispatch constrained by stochastic wind power availability and cost," vol. 25, no. 3, pp. 1705–1713, 2010.

[15] X.-F. Wang, Y.-H. Song, and M. Irving, *Modern Power Systems Analysis*. Springer, 2008.

[16] C.-R. Wang, H.-J. Yuan, Z.-Q. Huang, J.-W. Zhang, and C.-J. Sun, "A modified particle swarm optimization algorithm and its application in optimal power flow problem," in *Proc. Int Machine Learning and Cybernetics Conf*, vol. 5, pp. 2885–2889, 2005.

[17] J. G. Vlachogiannis and K. Y. Lee, "Economic load dispatch—a comparative study on heuristic optimization techniques with an improved coordinated aggregation-based pso," vol. 24, no. 2, pp. 991–1001, 2009.

[18] M. R. AlRashidi, M. F. AlHajri, and M. E. El-Hawary, "Enhanced particle swarm optimization approach for solving the non-convex optimal power flow," *World Academy of Science, Engineering and Technology*, vol. 62, pp. 651–655, 2010.

[19] J. Kennedy and R. Eberhart, "Particle swarm optimization," in *Proc. Conf. IEEE Int Neural Networks*, vol. 4, pp. 1942–1948, 1995.

[20] M. A. Abido, "Optimal power flow using particle swarm optimization," *International Journal of Electrical Power Energy Systems*, vol. 24, no. 7, pp. 563–571, 2002.

[21] P. N. Biskas, N. P. Ziogos, A. Tellidou, C. E. Zoumas, A. G. Bakirtzis, V. Petridis, and A. Tsakoumis, "Comparison of two metaheuristics with mathematical programming methods for the solution of opf," in *Proc. 13th Int Intelligent Systems Application to Power Systems Conf*, 2005.

[22] Z.-L. Gaing, "Particle swarm optimization to solving the economic dispatch

considering the generator constraints," vol. 18, no. 3, pp. 1187–1195, 2003.

[23] R. Boqiang and J. Chuanwen, "A review on the economic dispatch and risk management considering wind power in the power market," *Renewable and Sustainable Energy Reviews*, vol. 13, no. 8, pp. 2169–2174, 2009.

[24] I. G. Damousis, M. C. Alexiadis, J. B. Theocharis, and P. S. Dokopoulos, "A fuzzy model for wind speed prediction and power generation in wind parks using spatial correlation," vol. 19, no. 2, pp. 352–361, 2004.

[25] S. Li, D. Wunsch, E. O'Hair, and M. Glesselmann, "Using neural networks to estimate wind turbine power generation," in *Proc. IEEE Power Engineering Society Winter Meeting*, vol. 3, 2001.

[26] B. G. Brown, R. W. Katz, and A. H. Murphy, "Time series models to simulate and forecast wind speed and wind power," *Journal of Climate and Applied Meteorology*, vol. 23, no. 8, pp. 1184–1195, 1984.

[27] X. Liu, "Combined heat and power dispatch with wind power: A stochastic model and solutions," in *Proc. IEEE Power and Energy Society General Meeting*, pp. 1–6, 2010.

[28] J. Carta, P. Ramrez, and S. Velzquez, "A review of wind speed probability distributions used in wind energy analysis: Case studies in the canary islands," *Renewable and Sustainable Energy Reviews*, vol. 13, no. 5, pp. 933 – 955, 2009.

[29] X. Liu, W. Xu, and C. Huang, "Economic load dispatch with stochastic wind power: Model and solutions," in *Proc. IEEE PES Transmission and Distribution Conf. and Exposition*, pp. 1–7, 2010.

[30] J. Peschon, D. S. Piercy, W. F. Tinney, and O. J. Tveit, "Sensitivity in power systems," no. 8, pp. 1687–1696, 1968.

[31] P. R. Gribik, D. Shirmohammadi, S. Hao, and C. L. Thomas, "Optimal power flow sensitivity analysis," vol. 5, no. 3, pp. 969–976, 1990.

[32] N. D. Ghawghawe and K. L. Thakre, "Application of power flow sensitivity analysis and ptdf for determination of atc," in *Proc. Int. Conf. Power Electronics, Drives and*

Energy Systems PEDES '06, pp. 1–7, 2006.

[33] M. R. Patel, *Wind and Solar Power Systems*. CRC Press, 1999.

[34] J.-B. Park, K.-S. Lee, J.-R. Shin, and K. Y. Lee, "A particle swarm optimization for economic dispatch with nonsmooth cost functions," vol. 20, no. 1, pp. 34–42, 2005.

[35] A. I. Selvakumar and K. Thanushkodi, "A new particle swarm optimization solution to nonconvex economic dispatch problems," vol. 22, no. 1, pp. 42–51, 2007.

[36] W.-N. Lee, Y.-W. Jeong, J.-B. Park, J.-R. Shin, and K. Y. Lee, "Development of an educational simulator for particle swarm optimization and economic dispatch applications," in *Proc. Int. Conf. Intelligent Systems Applications to Power Systems ISAP 2007Lee2007*, pp. 1–6, 2007.

[37] B. Birge, "Psot - a particle swarm optimization toolbox for use with matlab," in *Swarm Intelligence Symposium, 2003. SIS '03. Proceedings of the 2003 IEEE*, pp. 182 – 186, april 2003.

[38] C. Moler, *Numerical computing with MATLAB*. Society for Industrial and Applied Mathematics, 2004.

[39] P. Wannakarn, S. Khamsawang, S. Pothiya, and S. Jiriwibhakorn, "Optimal power flow problem solved by using distributed sobol particle swarm optimization," in *Electrical Engineering/Electronics Computer Telecommunications and Information Technology (ECTI-CON), 2010 International Conference on*, pp. 445 –449, may 2010.

[40] O. Alsac and B. Stott, "Optimal load flow with steady-state security," *Power Apparatus and Systems, IEEE Transactions on*, vol. PAS-93, pp. 745 –751, may 1974.

APPENDICES

APPENDIX A

THE DATA FOR IEEE 30-BUS TEST SYSTEM

The data for IEEE 30-bus test system as following [40]:

Table A.1: Bus data of IEEE 30-bus test system

Bus No.	Bus Code*	Voltage (pu)	Angle (pu)	P_L (MW)	Q_L (MVAR)	$P_{G\#}$ (MW)	$Q_{G\#}$ (MVAR)	Q_{G}_low (MVAR)	Q_{G}_high (MVAR)	Q_{sh} (MVAR)
1	1	1.05	0	0	0	0	0	-20	250	0
2	2	1.04	0	21.7	12.7	80	0	-20	100	0
3	0	1	0	2.4	1.2	0	0	0	0	0
4	0	1	0	7.6	1.6	0	0	0	0	0
5	2	1.01	0	94.2	19	50	0	-15	80	0
6	0	1	0	0	0	0	0	0	0	0
7	0	1	0	22.8	10.9	0	0	0	0	0
8	2	1.01	0	30	30	20	0	-15	60	0
9	0	1	0	0	0	0	0	0	0	0
10	0	1	0	5.8	2	0	0	0	0	0
11	2	1.05	0	0	0	20	0	-10	50	0
12	0	1	0	11.2	7.5	0	0	0	0	0
13	2	1.05	0	0	0	20	0	-15	60	0
14	0	1	0	6.2	1.6	0	0	0	0	0
15	0	1	0	8.2	2.5	0	0	0	0	0
16	0	1	0	3.5	1.8	0	0	0	0	0
17	0	1	0	9	5.8	0	0	0	0	0
18	0	1	0	3.2	0.9	0	0	0	0	0
19	0	1	0	9.5	3.4	0	0	0	0	0
20	0	1	0	2.2	0.7	0	0	0	0	0
21	0	1	0	17.5	11.2	0	0	0	0	0
22	0	1	0	0	0	0	0	0	0	0
23	0	1	0	3.2	1.6	0	0	0	0	0
24	0	1	0	8.7	6.7	0	0	0	0	0
25	0	1	0	0	0	0	0	0	0	0
26	0	1	0	3.5	2.3	0	0	0	0	0
27	0	1	0	0	0	0	0	0	0	0
28	0	1	0	0	0	0	0	0	0	0
29	0	1	0	2.4	0.9	0	0	0	0	0
30	0	1	0	10.6	1.9	0	0	0	0	0

* Bus code: 1 for slack bus; 2 for PV bus; 0 for Load bus.
#These generators' Data are an initial guess.

Table A.2: Generators data of IEEE 30-bus test system

Gen. No.	a ($/MW^2.Hr)	b ($/MW.Hr)	c	P_G_low (MW)	P_G_high (MW)
1	0.00375	2	0	50	200
2	0.0175	1.75	0	20	80
5	0.0625	1	0	15	50
8	0.00834	3.25	0	10	35
11	0.025	3	0	10	30
13	0.025	3	0	12	40

Table A.3: Line data of IEEE 30-bus test system

Branch No.	From Bus	To Bus	R (pu)	X (pu)	B (pu)	Transformer (turnns ratio)	Ratings (MVA)
1	1	2	0.0192	0.0575	0.0264	1	130
2	1	3	0.0452	0.1852	0.0204	1	130
3	2	4	0.057	0.1737	0.0184	1	65
4	3	4	0.0132	0.0379	0.0042	1	130
5	2	5	0.0472	0.1983	0.0209	1	130
6	2	6	0.0581	0.1763	0.0187	1	65
7	4	6	0.0119	0.0414	0.0045	1	90
8	5	7	0.046	0.116	0.0102	1	70
9	6	7	0.0267	0.082	0.0085	1	130
10	6	8	0.012	0.042	0.0045	1	32
11	6	9	0	0.208	0	1.078	65
12	6	10	0	0.556	0	1.069	32
13	9	11	0	0.208	0	1	65
14	9	10	0	0.11	0	1	65
15	4	12	0	0.256	0	1.032	65
16	12	13	0	0.14	0	1	65
17	12	14	0.1231	0.2559	0	1	32
18	12	15	0.0662	0.1304	0	1	32
19	12	16	0.0945	0.1987	0	1	32
20	14	15	0.221	0.1997	0	1	16
21	16	17	0.0824	0.1923	0	1	16
22	15	18	0.1073	0.2185	0	1	16
23	18	19	0.0639	0.1292	0	1	16
24	19	20	0.034	0.068	0	1	32
25	10	20	0.0936	0.209	0	1	32
26	10	17	0.0324	0.0845	0	1	32
27	10	21	0.0348	0.0749	0	1	32
28	10	22	0.0727	0.1499	0	1	32
29	21	22	0.0116	0.0236	0	1	32
30	15	23	0.1	0.202	0	1	16
31	22	24	0.115	0.179	0	1	16
32	23	24	0.132	0.27	0	1	16
33	24	25	0.1885	0.3292	0	1	16
34	25	26	0.2544	0.38	0	1	16
35	25	27	0.1093	0.2087	0	1	16
36	28	27	0	0.396	0	1.068	65
37	27	29	0.2198	0.4153	0	1	16
38	27	30	0.3202	0.6027	0	1	16
39	29	30	0.2399	0.4533	0	1	16
40	8	28	0.0636	0.2	0.0214	1	32
41	6	28	0.0169	0.0599	0.0065	1	32

APPENDIX B

THE DATA FOR 6-BUS SYSTEM

The data for 6-bus system is originally taken form [39] but they are modified to include wind-powered generators. The data as follows:

Table B.1: Bus data of 6-bus system

Bus No.	Bus Code*	Voltage (pu)	Angle (pu)	P_L (MW)	Q_L (MVAR)	$P_{G\#}$ (MW)	$Q_{G\#}$ (MVAR)	Q_{G}_low (MVAR)	Q_{G}_high (MVAR)	Q_{sh} (MVAR)
1	1	1	0	66.67	13.33	0	0	0	0	0
2	2	1	0	66.67	13.33	188	0	0	0	0
3	2	1	0	66.67	13.33	40	0	0	0	0
4	2	1	0	66.67	13.33	24	0	0	0	0
5	0	1	0	66.67	33.33	0	0	0	0	0
6	0	1	0	66.67	6.67	0	0	0	0	0

* Bus code: 1 for slack bus; 2 for PV bus; 0 for Load bus.
# The generators' data are an initial guess.

Table B.2: Generators data of 6-bus system

Gen. No.	a ($/MW^2.hr)	b ($/MW.hr)	c	P_{G}_low (MW)	P_{G}_high (MW)
1	0.012	12	105	50	250
2	0.0096	9.6	96	50	250
3	0	8	0	0	40
4	0	6	0	0	40

Table B.3: Line data of 6-bus system

Branch No.	From Bus	To Bus	R (pu)	X (pu)	B/2 (pu)	Rating (MVA)
1	1	2	0.04	0.08	0.02	100
2	1	5	0.04	0.08	0.02	160
3	2	4	0.04	0.08	0.02	160
4	3	5	0.04	0.08	0.02	100
5	3	6	0.04	0.08	0.02	100
6	4	5	0.04	0.08	0.02	100
7	4	6	0.04	0.08	0.02	100

APPENDIX C

SENSITIVITY ANALYSIS FOR OPTIMAL POWER FLOW

C.1 INTRODUCTION

Earlier research on the application of sensitivity analysis in power system belongs to Peschon et al [30]. They introduced two methods. First one can be applicable to normal power flow problems for small changes in the variables such as active generation and second method considers the minimization of objective function satisfying some constraints such as power flow equation. Similar research was carried out by Gribik et al [31].

C.2 MATHEMATICAL FORMULATION

The method of calculating the sensitivities of voltages and currents are determined simultaneously, which are further used to determine the changes in power flows. Considering the generalized equations of the form [32]:

$$g(\mathbf{x},\mathbf{u},\mathbf{p}) = 0 \tag{C.1}$$

where g is $2N$ dimensional vector, and N is number of buses. The variables mentioned in equation (C.1) can be categorized as:

($\mathbf{x}$) are dependent (state) variables, these are the controlled variables and they are unknown. $\mathbf{x}$ is a $2N$ dimensional vector.

($\mathbf{u}$) are independent control variables, these are the operating variables or imposed variables of the system. $\mathbf{u}$ is an M dimensional vector.

($\mathbf{p}$) are parameter variables, these are uncontrollable variables and are normally specified in the power flow problem such as the admittance and the loads.

Depending upon the variables to be determined, the variables in the power flow problem can be selected as $\mathbf{x}$, $\mathbf{u}$ and $\mathbf{p}$. One might be interested in controlling K variables out of the $2N$ variables.

If $\mathbf{x}_0$, $\mathbf{u}_0$, and $\mathbf{p}_0$ are the initial state vectors, rewriting equation (C.1) as:

$$g(\mathbf{x}_0, \mathbf{u}_0, \mathbf{p}_0) = 0 \tag{C.2}$$

The changes $\Delta\mathbf{x}$ corresponding to small changes $\Delta\mathbf{u}$ and $\Delta\mathbf{p}$, will satisfy the new equations:

$$g(\mathbf{x}_0 + \Delta\mathbf{x}, \mathbf{u}_0 + \Delta\mathbf{u}, \mathbf{p}_0 + \Delta\mathbf{p}) = 0 \tag{C.3}$$

Expanding (C.3) by Taylor's series and neglecting higher order terms,

$$g(\mathbf{x}_0 + \Delta\mathbf{x}, \mathbf{u}_0 + \Delta\mathbf{u}, \mathbf{p}_0 + \Delta\mathbf{p}) = g(\mathbf{x}_0, \mathbf{u}_0, \mathbf{p}_0) + g_x\Delta\mathbf{x} + g_u\Delta\mathbf{u} + g_p\Delta\mathbf{p} \tag{C.4}$$

where, g_x, g_u and g_p are the partial derivatives of g with respect to x, u and p respectively and are given by:

$$g_x = \frac{\partial(g_1, g_2, ..., g_{2N})}{\partial(x_1, x_2, ..., x_{2N})} \tag{C.5}$$

where x_1, x_2,...,x_2N are the elements of $\mathbf{x}$.

$$g_u = \frac{\partial(g_1, g_2, ..., g_{2N})}{\partial(u_1, u_2, ..., u_M)} \tag{C.6}$$

where u_1, u_2,...,u_M are the elements of $\mathbf{u}$.

$$g_p = \frac{\partial(g_1, g_2, ..., g_{2N})}{\partial(p_1, p_2, ..., p_{2N})} \tag{C.7}$$

where p_1, p_2,...,p_{2N} are the elements of $\mathbf{p}$.

When changes are small, solution for $\Delta\mathbf{x}$ will be,

$$\Delta\mathbf{x} = \mathbf{S}_u\Delta\mathbf{u} + \mathbf{S}_p\Delta\mathbf{p} \tag{C.8}$$

where $\mathbf{S}_u$ and $\mathbf{S}_p$ are the sensitivities of $\mathbf{x}$ with respect to $\mathbf{u}$ and $\mathbf{p}$ respectively and are obtained as:

$$\mathbf{S}_u = -{g_x}^{-1} g_u \tag{C.9}$$

$$\mathbf{S}_p = -{g_x}^{-1} g_p \tag{C.10}$$

If $\mathbf{p}$ variables are not changed then (C.8) can be re-written as:

$$\Delta \mathbf{x} = \mathbf{S}_u \Delta \mathbf{u} \tag{C.11}$$

The set of dependent and independent variables can be chosen as per the system requirement and problem formulation. Some of the parameters of a type may belong to the set of dependent whereas remaining parameters of same type may belong to the set of independent variables. for instance, as bus voltages they might be considered as independent variables when they are at generator buses while they are considered dependent at load buses.

C.3 DETERMINATION OF VOLTAGE SENSITIVITIES AT BUSES

Power flow equations are comprising of 6 variables namely P, Q, V, δ ,Y and θ. All the variables can be assumed to be obtained or specified at the base condition. The variables Y and θ are normally specified and are constant. The other variables are not always constant and they are either specified or determined, depending upon the type of buses. The variables for which changes are specified are grouped as independent variables and the variables which are determined against these changes are grouped as dependent variables [32].

For the slack bus, V and δ are specified and P and Q are subjected to change. For generator bus, P and V are specified and Q and δ are subjected to change. For load buses, P and Q are specified and V and δ are changed. Now consider the power system of N buses and B branches. Power flow equations can be described by (2.17 , 2.18). There are $2N$ set of equations and a set of $2N$ variables can be selected as state variables ($\mathbf{x}$) and remaining as control variables ($\mathbf{u}$).

Consider that only M control variables are changed and for these changes, it is desired to obtain the changes in the real and reactive power at slack buses, reactive power and angles at generator buses and voltages and angles at load buses. TN hen, the power flow

equations can be written as following:

$$g(V_i, V_j, \delta_i, \delta_j, P_i, Q_i, Y_{ij}, \theta_{ij}) = 0 \tag{C.12}$$

Let

$P_{sl}, P_G, P_L \in P_i$

$Q_{sl}, Q_G, Q_L \in Q_i$

$V_{sl}, V_G, V_L \in V_i$

Grouping the variables of (C.12) as g

$$\mathbf{x} = [P_{sl}, Q_{sl}, Q_G, \delta_G, V_L, \delta_L] \tag{C.13}$$

$$\mathbf{u} = [V_{sl}, \delta_{sl}, P_G, V_G, P_L, Q_L] \tag{C.14}$$

$$\mathbf{p} = Y_{ij},\ \theta_{ij} \tag{C.15}$$

From (C.11), the changes in dependent variables can be obtained

$$[\Delta P_{sl}, \Delta Q_{sl}, \Delta Q_G, \Delta\delta_G, \Delta V_L, \Delta\delta_L] = \mathbf{S}[\Delta V_{sl}, \Delta\delta_{sl}, \Delta P_G, \Delta V_G, \Delta P_L, \Delta Q_L] \tag{C.16}$$

where $\mathbf{S}$ is the sensitivity matrix of order $2N$x$2N$ and can be obtained as given by (C.9). For slack bus and generator buses following substitution can be made in (C.16):

$$\Delta V_{sl} = \Delta V_G = \Delta\delta_{sl} = 0 \tag{C.17}$$

After determining the changes in the load bus voltages, load bus angles and generator bus angles from (C.16) and with the substitutions from (C.17) all the bus voltages and angles can be arranged as:

$$[\Delta\mathbf{V}, \Delta\boldsymbol{\delta}] = [\Delta V_{sl}, \Delta V_G, \Delta V_L, \Delta\delta_{sl}, \Delta\delta_G, \Delta\delta_L] \tag{C.18}$$

C.4 DETERMINATION OF CURRENT SENSITIVITIES IN THE LINES

It is well known that the changes in voltage angles and voltage magnitudes are related to branch currents I_{ij} fig:cdffig:cdf[32]. These currents in complex form can be expressed as:

$$I_{ij} = Y_{ij}[V_i(cos\delta_i + jsin\delta_i) - V_j(cos\delta_j + jsin\delta_j)] \tag{C.19}$$

Where $Y_{ij} = |Y_{ij}|\angle\theta_{ij}$ and $I_{ij} \in B$, since B is the number of branches. Equation (C.19) can be written in the form:

$$g_{ij}(I_{ij}, Y_{ij}, \theta_{ij}, V_i, V_j, \delta_i, \delta_j) = 0 \tag{C.20}$$

Grouping the variables of (C.20) as

$\mathbf{x} = I_{ij}$

$\mathbf{u} = V_i, V_j, \delta_i, \delta_j$ (i.e. V and δ variables at all buses)

$\mathbf{p} = |Y_{ij}|,\ \theta_{ij}$.

Sensitivities of I_{ij} for the changes in $V_i, V_j, \delta_i, \delta_j$ can be obtained from (C.11) as:

$$\Delta I_{ij} = \mathbf{R}[\Delta\mathbf{V}, \Delta\boldsymbol{\delta}] \tag{C.21}$$

where $\mathbf{R}$ is sensitivity matrix obtained by (C.9) which is given as:

$$\mathbf{R} = -g_{ijx}^{-1}\, g_{iju} \tag{C.22}$$

With g_{ijx} is Jacobian of g_{ij} with respect to $\mathbf{x}$ (i.e. I_{ij}).

While g_{iju} is Jacobian of g_{ij} with respect to $\mathbf{u}$ (i.e. $V_i, V_j, \delta_i, \delta_j$) Substituting from (C.18), (C.22) can be rewritten as:

$$[\Delta I_{ij}]_{B\times 1} = [\mathbf{R}]_{B\times 2N}[\Delta V_{sl}, \Delta V_G, \Delta V_L \Delta\delta_{sl}, \Delta\delta_G, \Delta\delta_L]_{2N\times 1} \tag{C.23}$$

Where $\Delta V_{sl} = \Delta V_G = \Delta\delta_{sl} = 0$.

APPENDIX D

FLOWCHARTS OF MATLAB CODE

The Matlab code which is used for solving Optimal Power Flow is long and has several nested functions, as a result of that Matlab code is summarized in the following flowcharts:

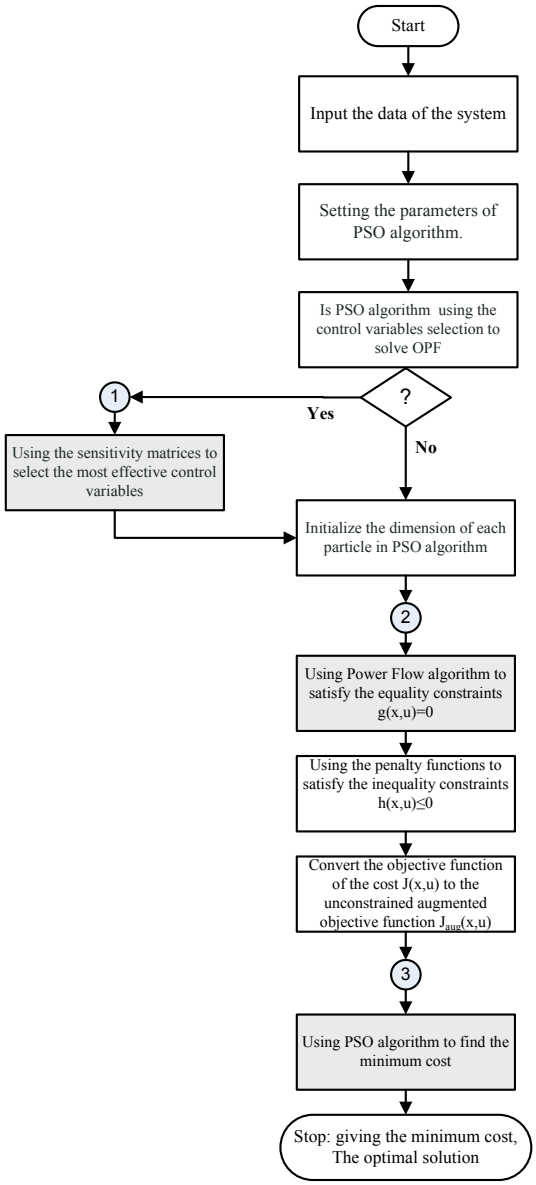

Figure D.1: Flowchart of the main OPF algorithm

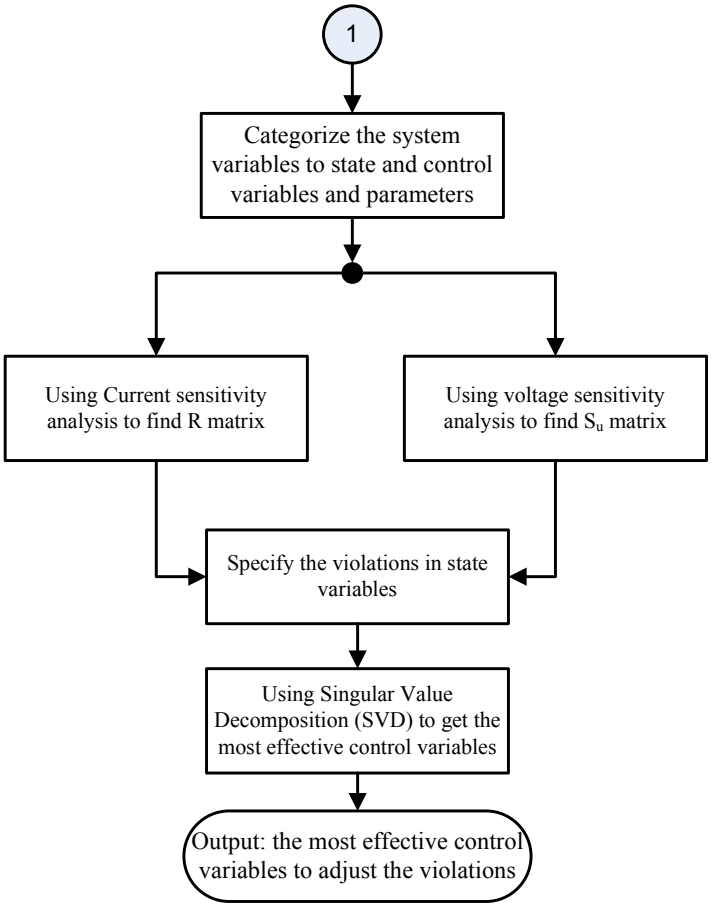

Figure D.2: Flowchart of the sensitivity analysis for OPF

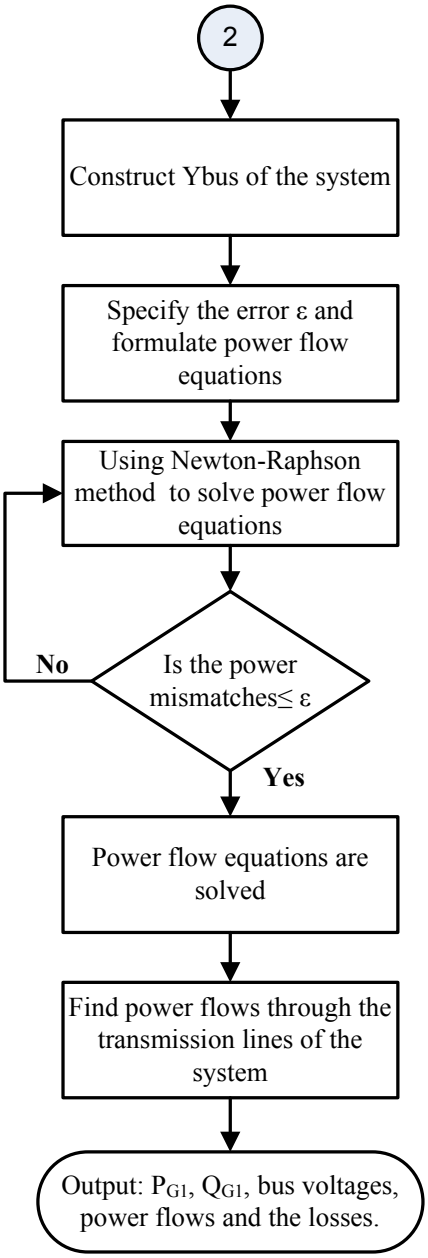

Figure D.3: Flowchart of Power flow algorithm

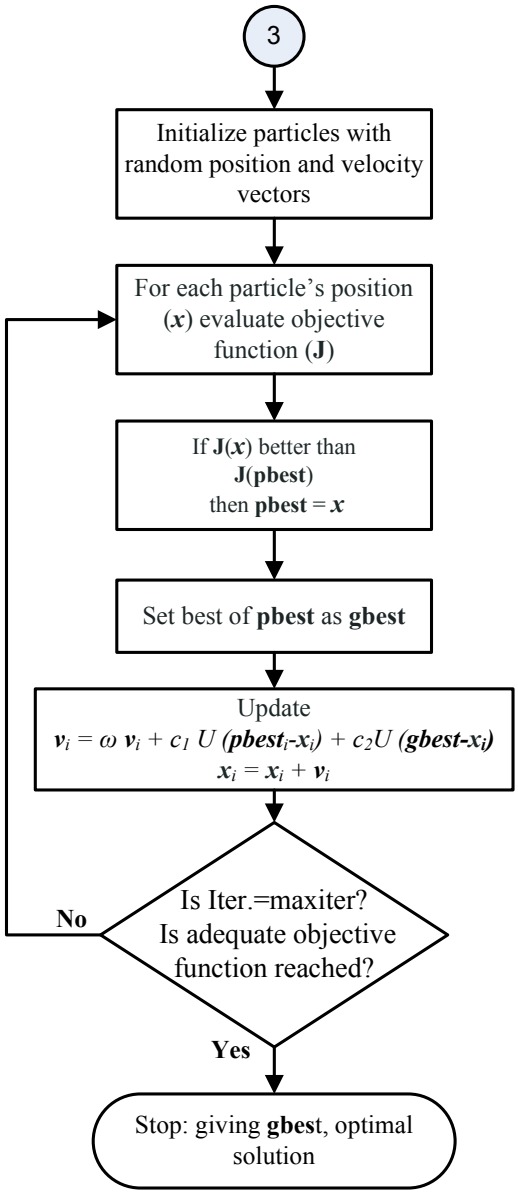

Figure D.4: Flowchart of PSO algorithm

VITA

Graduate School
Southern Illinois University

Mohamed A. Abuella

Email address: mohammedabuella@siu.edu

Higher institute of Industry, Misurata, Libya
Bachelor of Technology, Electric Power Systems, February 2008

Scholarship from Libyan Higher Education Ministry
Member of Institute of Electrical and Electronics Engineers
Member of Golden Key International Honor Society. Research Paper Title:

STUDY OF PARTICLE SWARM FOR OPTIMAL POWER FLOW IN IEEE BENCHMARK SYSTEMS INCLUDING WIND POWER GENERATORS

Major Professor: Dr. C. Hatziadoniu